Evaluating the adaptive potential of the European eel: is the immunogenetic status recovering?

Miguel Baltazar-Soares, Seraina E. Bracamonte, Till Bayer, Frédéric J.J. Chain, Reinhold Hanel, Chris Harrod, Christophe Eizaguirre

The recent increased integration of evolutionary theory into conservation programs has greatly improved our ability to protect endangered species. A common application of such theory links population dynamics and indices of genetic diversity, usually estimated from neutrally evolving markers. Some studies however have suggested that highly polymorphic adaptive genes, such as the immune genes of the Major Histocompatibility Complex (MHC), might be more sensitive to fluctuations in population dynamics. As such, the combination of neutrally- and adaptively-evolving genes may be informative in populations where reductions in abundance have been documented. The European eel (Anguilla anguilla) underwent a drastic and well-reported decline in abundance in the late 20th century and still displays low recruitment. Here we compared genetic diversity indices estimated from neutral (mitochondrial DNA and microsatellites) and adaptive markers (MHC) between two distinct generations of European eels. Our results revealed a clear discrepancy between signatures obtained for each class of markers. Although mtDNA and microsatellites showed no changes in diversity between the older and the younger generations, MHC diversity revealed a contemporary drop followed by a recent increase. Our results suggest ongoing gain of MHC genetic diversity resulting from the interplay between drift and selection and ultimately increasing the adaptive potential of the species.

Evaluating the adaptive potential of the European eel: is the immunogenetic status recovering?

Miguel Baltazar-Soares[1], Seraina E. Bracamonte[1, 2], Till Bayer[1], Frédéric J.J. Chain[3], Reinhold Hanel[4], Chris Harrod[5], Christophe Eizaguirre[6]

[1]GEOMAR Helmholtz Centre for Ocean Research Kiel, Düsternbrooker Weg 20, 24105 Kiel, Germany

[2]Leibniz-Institute of Freshwater Ecology and Inland Fisheries, Muggelseedamm 310, 12587 Berlin, Germany

[3]Department of Biology, McGill University, 1205 avenue Docteur Penfield, Montréal, Québec, H3A 1B1, Canada

[4]Thunen-Institute of Fisheries Ecology, Palmaille 9, 22767 Hamburg, Germany

[5]Universidad de Antofagasta, Instituto de Ciencias Naturales Alexander von Humboldt, Avenida Angamos 601, Antofagasta, Chile

[6]School of Biological and Chemical Sciences, Queen Mary University of London, Mile End Road, London E1 4NS, UK

Abstract

The recent increased integration of evolutionary theory into conservation programs has greatly improved our ability to protect endangered species. A common application of such theory links population dynamics and indices of genetic diversity, usually estimated from neutrally evolving markers. Some studies however have suggested that highly polymorphic adaptive genes, such as the immune genes of the Major Histocompatibility Complex (MHC), might be more sensitive to fluctuations in population dynamics. As such, the combination of neutrally- and adaptively-evolving genes may be informative in populations where reductions in abundance have been documented. The European eel (*Anguilla anguilla*) underwent a drastic and well-reported decline in abundance in the late 20th century and still displays low recruitment. Here we compared genetic diversity indices estimated from neutral (mitochondrial DNA and microsatellites) and adaptive markers (MHC) between two distinct generations of European eels. Our results revealed a clear discrepancy between signatures obtained for each class of markers. Although mtDNA and microsatellites showed no changes in diversity between the older and the younger generations, MHC diversity revealed a contemporary drop followed by a recent increase. Our results suggest ongoing gain of MHC genetic diversity resulting from the interplay between drift and selection and ultimately increasing the adaptive potential of the species.

Introduction

Preserving natural biodiversity while allowing species to maintain their adaptive potential is a major challenge in modern conservation biology (Frankham et al. 2002). Anthropogenic activities impact global ecosystems and reduce population sizes of species, whether by shrinking or fragmenting available habitats, overexploitation, or disruption of population dynamics (Allendorf et al. 2008; England et al. 2010; Thomas et al. 2004). Small populations are more vulnerable to environmental, demographic and genetic processes (Keith et al. 2008). Genetic factors are particularly important as they may not manifest immediately after population reduction but their effects persist in the population even if the population size recovers to otherwise sustainable levels, e.g. through bottleneck effects (Spielman et al. 2004). Populations display complex evolutionary dynamics and evolutionary genetics offers ideal framework for conservation biologists to monitor population changes and viability (Hendry et al. 2011). Although genetic studies applied to wild populations of non-model species have largely focused on the analysis of neutrally evolving loci (see (McMahon et al. 2014)), conservation managers have expanded their toolbox to include screening of adaptive loci (Hendry et al. 2011). Such measures are required to fill knowledge gaps regarding species' evolutionary and adaptive potential (Eizaguirre & Baltazar-Soares 2014).

The genes of the Major Histocompatibility Complex (MHC) have repeatedly been shown to be suitable candidates to evaluate the immune adaptive potential of endangered populations (Sommer 2005; Stiebens et al. 2013b). This highly polymorphic (high heterozygosity and gene duplications), multigene family (Apanius et al. 1997; Klein et al. 2007) plays a decisive role in

59 controlling the vertebrate adaptive immune system by presenting self- and pathogen-derived
60 peptides to T-cells (Janeway et al. 2005). Pathogen-mediated selection is acknowledged to be
61 one of the primary factors of balancing selection maintaining the extreme MHC polymorphism
62 in a population (Eizaguirre et al. 2012a; Piertney & Oliver 2006; Spurgin & Richardson 2012).
63 Therefore, investigating shifts in MHC allele frequencies (Eizaguirre et al. 2012b) may be a
64 particularly informative tool as an indirect way to detect the emergence of diseases (Sommer
65 2005). Similarly, examining how MHC genetic diversity fluctuates in parallel with the incidence
66 of diseases or parasites can provide indirect evidence for the impact of those selective agents
67 on the dynamics of the host population (McCallum 2008). Lastly, MHC genes have also shown
68 to be informative of demographic events, particularly when selection plays an important role in
69 population reductions (Sutton et al. 2011).

70 The European eel is a highly migratory, semelparous fish whose spawning grounds are located
71 in the Sargasso Sea and whose foraging grounds cover coastal, mixohaline and freshwater
72 habitats (Harrod et al. 2005) across much of Europe and even extend to North Africa and the
73 Levantine coast. The post-hatching early larval transport is first facilitated by local currents in
74 the Sargasso sea, connecting the spawning area with the Gulf Stream (Baltazar-Soares et al.
75 2014), and by the North Atlantic gyre, that completes the larval migration to the continental
76 shelf (Bonhommeau et al. 2008; Kettle et al. 2008b; Munk et al. 2010). Once larval eels enter
77 shelf waters, they undergo a series of substantial changes in morphology and physiology:
78 individuals become glass eels, with a fusiform, transparent body that facilitates active
79 swimming towards coastal waters (Miller 2009). The duration of the continental life stage varies
80 on the location of growth habitats, and may last from as little as two years (EIFAAC/ICES 2013)

to several decades prior to metamorphose into silver eel. At this stage, energetic reserves are collected to allow sexual maturation and the long spawning migration back to the Sargasso Sea (Tesch 2003).

Although the number of glass eels arriving at continental coasts across Europe experienced a first drop in the 1960s, the major recruitment collapse occurred at the beginning of the 1980s (EIFAAC/ICES 2011). For the subsequent three decades, the recruitment of glass eels has remained as low as 1 to 10% of the values prior to the 1980s (EIFAAC/ICES 2011). The low recruitment regime is hypothesized to have resulted from multiple impairing factors including productivity changes in the Sargasso Sea (Friedland et al. 2007), habitat degradation including river regulation, pollution and reduced freshwater habitats (Prigge et al. 2013; Robinet & Feunteun 2002), changes in oceanic currents (Baltazar-Soares et al. 2014; Kettle et al. 2008a), introduction and spread of diseases, such as the EVEX (Van Ginneken et al. 2005) and the swim bladder parasite *Anguillicola crassus* (Kirk 2003), resulting in a severe lack of spawners (Dekker 2003). Experimental studies focusing on this invasive nematode for instance revealed that the European eel is unable to mount an effective immune response, thus becoming particularly susceptible to infection (Knopf 2006).

The European eel is currently considered a single panmictic population (Als et al. 2011; Pujolar et al. 2014), even though punctual deviations from panmixia have been reported (Baltazar-Soares et al. 2014; Dannewitz et al. 2005; Wirth & Bernatchez 2001). While the vast majority of genetic studies have focused on solving the population structure of the species, few have tried to determine the impact of the recruitment decline on the species' genetic diversity (Pujolar et

al. 2011; Pujolar et al. 2013; Wirth & Bernatchez 2003). Studies that aimed at doing so have evaluated neutrally evolving genetic markers. In 2003, Wirth and Bernatchez (Wirth & Bernatchez 2003) analyzed 7 microsatellite loci in 611 European eel individuals and reported no measurable signature of the 1980s recruitment decline. In 2011, Pujolar and coworkers (Pujolar et al. 2011) analyzed the diversity of 22 microsatellite markers on 346 individuals. Again, genetic signature of a population reduction was absent. It was therefore suggested that the 1980s decline, although marked in terms of population biology was not sufficiently extreme to affect the diversity of these polymorphic and neutrally evolving loci (Pujolar et al. 2011). Employing a genome-wide reduced representation sequencing technique (RAD) – that identified in its vast majority neutral markers – Pujolar et al. (Pujolar et al. 2013) did not detect either evidence for a recent decline of genetic diversity to be associated with the drastic drop in recruitment (Pujolar et al. 2013).

Here, we expand on these studies detailing an extensive evaluation of the current genetic status of the European eel species, which includes 1) screening of both neutral and adaptive markers and 2) a temporal approach directly comparing two distinct generations of eels. A temporal approach is regarded as a key requirement when investigating the signature of demographic events on genetic diversity in a wild population (Sutton et al. 2015). Specifically for the eel system, evaluating genetic diversity in two distinct, non-overlapping age cohorts is important since the major component of genetic distribution of nuclear markers in this species seems to relate to different age cohorts (Dannewitz et al. 2005).

Material and methods

Study scheme

A total of 683 eels were analyzed in this study, 202 of which corresponded to mature silver eels caught in freshwater while undertaking their spawning migration. The other 481 individuals were glass eels collected from 2009 to 2012 immediately upon their arrival in coastal waters (Fig. S1). Number of individuals per sampling site, year of capture, developmental stage, and geographical locations can be found in Table 1. Note, we mostly sampled in one catchment per country and used countries' acronyms to refer to the locations where the specimens were collected. All samples were included in the analyses of mtDNA and microsatellites. Although the main objective of this work was to evaluate the genetic status of the eel species on a temporal scale, we also analyzed spatial patterns of genetic differentiation for comparison with previously published studies (Als et al. 2011; Maes & Volckaert 2002; Pujolar et al. 2014; Wirth & Bernatchez 2001).

Amongst the 683 individuals, 327 were sequenced at the exon 2 of the MHC class II B gene. This number was achieved as a compromise between costs of 454 sequencing and the need to provide sample sizes sufficient to provide a robust screen for spatial and temporal patterns of local adaptation. Locations and respective sample sizes of fish screened for the MHC gene are highlighted in Fig. S2. Temporal analyses were performed after dividing the dataset in two distinct age groups: the older "*silver eels*" age group and the younger "*glass eels*" group. The first group included individuals born soon after the drop in recruitment (late 1990s and early 2000s) while the second group consisted of very recently recruited individuals (2009 onwards) (ICES 2015). DNA was extracted from fin clips ("*silver eels"*) or tail clips (*"glass eels"*) with

Qiagen DNeasy Kit © Blood and Tissue kit (Hilden, Germany) following the manufacturer's protocol.

Neutrally evolving mitochondrial marker

Genetic estimates of diversity, population differentiation and demography

All 683 glass eels were sequenced using Sanger sequencing for the mitochondrial NADH dehydrogenase 5 (*ND5*) exactly replicating (Baltazar-Soares et al. 2014). Haplotype diversity (*Hd*) and nucleotide diversity (π) were calculated for each sampling location in DnaSP v5 (Librado & Rozas 2009). Genetic structure was estimated using Arlequin v3.5 with 10.000 permutations (Excoffier & Lischer 2009). Moment-based demographic parameters that test for changes in effective population size were calculated for each sampling location in DnaSP v5 under the assumption of mutation-drift equilibrium. Tajima's *D* (Tajima 1989) and raggedness' *r* (Rogers & Harpending 1992) were also calculated in DnaSP v5. Ninety-five percent confidence intervals were estimated through coalescence simulations using 1.000 permutations. We evaluated the nucleotide mismatch pairwise distributions within each geographical location (Rogers & Harpending 1992). These distributions were compared to expected distributions under a constant population size and sudden population expansion (Librado & Rozas 2009).

Neutrally evolving nuclear markers

Genetic estimates of diversity, differentiation and demography amongst freshwater locations

163 All samples were genotyped for twenty-two microsatellite loci optimized from previous studies
164 (Als et al. 2011; Pujolar et al. 2009; Wielgoss et al. 2008b). Amplification took place in four PCR
165 multiplexes of four to six loci each. Specifically: multiplex A – 55°C annealing temperature –
166 included CT77, CT87, CA55, CA58, CT68, and AJTR-37; multiplex B - 55°C annealing temperature
167 – included CT82, CT76, CT89, CT59, CA80, and CT53; multiplex C - 60°C annealing temperature
168 – included C01, M23, AJTR-45, AJTR27, I14, and O08; multiplex D - 60°C annealing temperature
169 – included AJTR-42, B09, B22, and N13. All reactions were performed in a total volume of 10 µl
170 and followed the QIAGEN© Multiplex PCR kit's recommendations. Genotyping was performed
171 on an ABI© 3100 Genetic Analyzer. Alleles were called in GENEMARKER© v. 1.91 (Softgenetics
172 LLC, State College, PA).

173 Nei's unbiased heterozygosity (*He*), observed heterozygosity (*Ho*) and F_{IS} were calculated for
174 each sampling location in GENETIX (1.000 bootstrap, (Belkir K 1999)). Rarefied allelic richness
175 (*Ar*) was calculated for each sampling location in HP-RARE v1.0 (Kalinowski 2005). Genetic
176 structure amongst sampling locations was inferred through pairwise comparisons in Arlequin
177 v3.5 and Bayesian clustering in STRUCTURE v2.3.3 (Pritchard et al. 2000). STRUCTURE was run
178 assuming a maximum number of possible groups of K = 26, i.e. representing the sum of all
179 spatial and temporal partitions of our sample, with 10 000 MCMC repeats after a 1000 burn-in
180 while assuming an admixture model with correlated allele frequencies. Three iterations were
181 performed for each K.

182 Genetic signatures of a bottleneck were tested for each location using the tests available in
183 BOTTLENECK (Cornuet & Luikart 1996). These methods are sensitive to recent and severe

reductions on effective population size (N_e) (Cornuet & Luikart 1996). A two-phase mutation model was assumed with 10% of the loci allowed to evolve through stepwise mutation (Kimura & Ohta 1978). Allele frequency distributions were also calculated for each location.

Genetic estimates of diversity, differentiation and demography – inter-generation level

In order to compare genetic diversity and demographic histories between the two cohorts and to avoid sampling bias from disproportionate number of samples in the two eel age groups ("*glass eels*" n=481 and "*silver eels*" n=202), we performed 10 rounds of re-sampling of the data without replacement using PopTools (Hood 2010), hereafter referred to as "replicates". Replicates were performed based on 50 individuals. This standardization is critical to validate future comparisons, as it has been long acknowledged that sample size affects the detection of genetic signatures of recent bottlenecks (Luikart et al. 1998) and the estimation of effective population size (Waples & Do 2010).

Deviations from Hardy-Weinberg equilibrium (HWE) were calculated for each replicate in Arlequin v3.5 (10 000 permutations). Nei's unbiased heterozygosity (*He*), observed heterozygosity *(Ho)*, allelic richness (*Ar*) and F_{IS} were calculated and compared between groups of replicates, i.e. "*glass eels*" and "*silver eels*", with two-sided t-tests in FSTAT (1000 permutations) (Goudet 1995). The distribution of genetic variance between "*glass eels*" and "*silver eels*" was assessed with an analysis of molecular variance (AMOVA, Arlequin v3.5) amongst groups of replicates. Demographic history was inferred using two approaches. First, we evaluated the possible genetic signature of the recent population decline using BOTTLENECK

(1000 iterations) for each age group as previously described. Second, we estimated the effective population size (N_e) of each replicate of "*silver eels*" and "*glass eels*" using the linkage-disequilibrium method implemented in NeEstimator V2.01 (Do et al. 2014). We utilized P_{crit} = 0.05, since lower P_{crit} can overestimate *Ne* (Waples & Do 2008). All estimates were obtained with the composite Burrows method (Weir 1990). The unweighted harmonic mean was calculated for each group according to the following equation: $\widehat{N}_e = \frac{j}{\sum_{i=1}^{j}(1/N_{e(i)})}$ where *j* is the number of replicates, *i* is a given replicate and $N_{e(i)}$ is the N_e estimate of the *ith* replicate (Waples & Do 2010).

Adaptive marker: diversity and demography of the MHC

We amplified the exon 2 of the MHC class II gene that encodes for the peptide-binding groove of the molecule following protocols optimized for the European eel (Bracamonte et al. 2015). We used the forward primer AaMHCIIBE2F3 (5´- AGTGYCGTTTCAGYTCCAGMGAYCTG-3´) and reverse primer AaMHCIIBE2R2 (5´- CTCACYTGRMTWATCCAGTATGG-3´) which allow the amplification of different allelic lineages of the MHC class II β genes (Bracamonte et al. 2015). Sequencing was performed on a 454© platform at LGC genomics (Belgium) following (Stiebens et al. 2013a; Stiebens et al. 2013b). Briefly, two independent reactions were prepared for each individual. After a first PCR of 20 cycles, a reconditioning step (dilution 1:5) was performed, and the template was used for a second PCR of 20 cycles. The reconditioning step combined with independent reactions was shown to significantly decrease the number of PCR artifacts (Lenz & Becker 2008) and facilitate allele call (Stiebens et al. 2013a). The second set of PCR was performed using the specific MHC primers extended by the 454 adaptors and a 10 bp individual

tag. Allele calling and respective assignment to individuals followed (Stiebens et al. 2013a; Stiebens et al. 2013b) and primarily relied on matching alleles present in both independent reactions (Sommer et al. 2013). Genotyping using this method has previously been compared to Sanger sequencing and showed its high accuracy (Bracamonte et al. 2015). Even though variants may stem from different loci, we will refer to them as alleles hereafter.

Individual MHC allele numbers detected from the different paralogs, nucleotide diversity, and individual average nucleotide p-distance (Eizaguirre et al. 2012a) were calculated for each sampling location and for each group, i.e. "*silver eels*" and "*glass eels*", in DnaSP v5 and using custom Perl scripts. MHC allele pools were compared amongst sampling locations and between "*silver eels*" and "*glass eels*" with analyses of similarity (ANOSIM) using Primer v6 (Clarke 1993) following (Eizaguirre et al. 2011) 1000 permutations). Correlation between MHC divergence and neutral structure was calculated using a Mantel test between pairwise F_{ST} matrices (mtDNA and microsatellites) and pairwise Bray-Curtis similarity matrices (MHC).

Minimum number of recombination events (*Rm*) and estimates of recombination rate (R) were calculated in DnaSP v5 (Hudson & Kaplan 1985), as well as the relative (R/θ) contribution of recombination (R) and point mutations (θ) in the generation of genetic diversity (Reusch & Langefors 2005). Gene conversion was investigated using ψ that measures the probability of a site to be informative for a conversion event (ψ>0, (Betran et al. 1997)) between "*glass eels*" and "*silver eels"*, using a sliding window method (window length = 2, step size = 1) implemented in DnaSP v5.

246 In order to test for the mode of evolution of the MHC in *A. anguilla*, overall positive selection
247 was estimated with a Z-test implemented in MEGA v5 (Tamura et al. 2011). We tested for signs
248 of codon-specific positive selection using maximum likelihood site models with CODEML
249 implemented in PAML v4.4 (Yang 2007) and the mixed effects model of evolution (MEME)
250 (Murrell et al. 2012) implemented in the Datamonkey web server (Delport et al. 2010; Pond &
251 Frost 2005). The maximum likelihood procedures evaluate heterogeneous ratios (ω) among
252 sites by applying different models of codon evolution. Three likelihood-ratio tests of positive
253 selection were performed comparing the models M1a (nearly neutral) *vs* M2a (positive
254 selection), M7 (ß) *vs* M8 (ß +ω), and M8a (ß +ω=1) *vs* M8 (Yang 2007). In the models M2a and
255 M8, positively selected sites are inferred from posterior probabilities calculated by the Bayes
256 inference method (Yang et al. 2005). We further tested for sites that experienced episodic
257 events of positive selection by using MEME. This model considers that ω varies between sites
258 (fixed effect), and between branches at a site (random effect) (Murrell et al. 2012). The null
259 expectation is that all branches have $\omega < 1$. In short, this model allows each site to have its own
260 selection history, contrary to fixed effect models (as the ones implemented in CODEML) that
261 assume constant selective pressures within a branch (Murrell et al. 2012).

262 To assume selection as the main evolutionary mechanism responsible for changes in genetic
263 diversity, sites under positive selection were concatenated for downstream analyses (Positively
264 Selected Sites, PSS). Theoretically, sites interacting with parasite-derived antigens are expected
265 to be under positive selection while other sites, within the same exon, may evolve differently
266 but still maintain the integrity of the MHC molecules. Therefore, we also concatenated the
267 remaining sites (nPSS) and performed identical analyses as for the PSS. Nucleotide mismatch

pairwise distributions were calculated for PSS and nPSS of both "*silver eels*" and "*glass eels*" under the assumptions of a constant population size and sudden expansion using DnaSP v5. The historical profile of MHC genetic diversity was investigated with Bayesian skyline plots (BSP) (Drummond et al. 2005) in BEAST v1.8 (Drummond & Rambaut 2007). Although these statistical procedures are often used to infer demographic events based on fluctuations of neutral genetic diversities, they have also been used to estimate the strength of adaptive evolution at the organism level (Bedford et al. 2011), and of functional genomic regions (Padhi & Verghese 2008).

Because of several expected characteristics of the MHC, including a deviation from a neutral mode of evolution, recombination or gene conversion events (Spurgin et al. 2011) and trans-species polymorphism (Lenz et al. 2013) that also occurs in this species (Bracamonte et al. 2015) as well as the existence at least three loci (Bracamonte et al. 2015), we did not attempt to associate the substitution rate to a clock-calibrated evolution. As such, we fixed a molecular clock and assumed three different mutation rates: 0.2, 1 (the default parameter) and 5 substitutions per time unit respectively. The substitution model was chosen in jModeltest (Tamura-Nei: Tn93) (Darriba et al. 2012; Guindon & Gascuel 2003) and also inserted as parameter in BEAST's runs. Markov chain run was set to a length of 1×10^8. The historical profile of MHC diversity was reconstructed for PSS and nPSS of both "*silver eels*" and "*glass eels*". Piecewise constant skyline model allowing for five skyline groups were used in three independent MCMC runs to verify consistence in parameter space. We then compared the marginal probability distributions of several parameters amongst the runs. Lastly, we

constructed lineage-through-time plots. These plots reflect accumulation of lineages through time translated for a given dated phylogeny (Nee et al. 1992).

Results

Neutrally evolving mitochondrial DNA

Molecular indices, population structure and demography amongst sampling locations

Analyses of 355 bp of the mtDNA *ND5* in 683 European eels revealed 102 haplotypes including 73 singletons (Data S1). Forty-eight randomly picked singletons were verified by independent extraction, amplification and re-sequencing to eliminate possible risks of sequencing errors. After we eliminated the possibility of sequencing errors (48 out of 48 singletons were verified by independent sequencing) we included all 73 singletons in the subsequent analyses. Amongst sampling locations, haplotype diversity ranged between 0.575 (BU) and 0.934 (GL). Nucleotide diversity ranged between 0.003 (G_SPA) and 0.008 (GL), with an average of 0.005 (± 0.001) amongst sampling locations (Table 1). Pairwise F_{ST} comparisons computed from haplotype frequencies amongst the 26 geographically confined groups revealed 17 significant pairwise differentiations however none passed corrections for multiple tests following the false discovery rate (threshold p = 0.013 for 26 tests (Narum 2006)). All results are shown in Table S1.

Tajima's *D* values were negative amongst almost all sampled locations, suggestive of population expansion or of population subdivision (Tajima 1989). The three exceptions were GER

(Germany), which belongs to a closed system, the Schwentine river, where recruitment is solely mediated by stocking (Prigge et al. 2013), as well as G_TITA (Italy) and G_WENG (England), where the values might reflect artificial stochasticity due to low sample sizes. Mismatch distribution analyses performed at the population level showed the typical pattern of a historical population expansion where the peak differs from zero (Rogers & Harpending 1992), Fig. 1a).

Molecular indices, population structure and demography between generations

Haplotype diversity and genetic diversity between "*silver eels*" and "*glass eels*" were very similar: $Hd_{\text{silver eels}} = 0.821$, $Hd_{\text{glass eels}} = 0.842$; $\pi_{\text{silver eels}} = 0.0048$, $\pi_{\text{glass eels}} = 0.0049$. No evidence for temporal genetic structure based on haplotype frequency distributions was detected between these groups, $F_{ST}=0.000$, $p=0.138$. Both groups also had negative and significant Tajima indices: $D_{\text{silver eels}} = -2.053$, $D_{\text{glass eels}} = -2.357$, both $p<0.05$ (Table 2). Mismatch distribution analyses revealed that both "*silver eels*" and "*glass eels*" display the distribution of expanding populations, suggesting that the overall pattern is not driven by a single generation and has a true biological origin visible in both cohorts (Fig. 2).

Neutrally evolving nuclear markers

Molecular indices, population structure and demography amongst locations

Across populations, *He* ranged between 0.687 (G_NIRL) and 0.758 (PT), *Ho* between 0.557 (G_TITA) and 0.667 (DK) and the average number of alleles per locus varied between 3.546 (G_VFRA) and 15.773 (G_AD2012). Allelic frequencies are reported in Data S2. F_{IS} varied between 0.0380 (G_NIRL) and 0.254 (Q) (Table S1). Even though F_{ST} estimates are very low, pairwise comparisons revealed 7 statistically significant pairwise comparisons after correcting for multiple testing (Table S1). Since six of those included comparisons between locations with low sample size, i .e. G_NIRL, G_WENG, G_TITA or G_BNIRL, the significance could be attributed to stochasticity due to low sample sizes. STRUCTURE analyses did not show any signs of population clustering as expected under the weak observed differentiation (Fig. S3).

None of the sampled locations showed either heterozygote excess or a mode shift in allele frequencies, genetic signatures characteristic of population bottlenecks (Fig. 1b).

Molecular indices, structure and demography between generations

Twenty-one loci were used to analyze “silver eels” and “glass eels” as locus AjTr-45 consistently deviated from Hardy-Weinberg equilibrium in all “*silver eels*” replicates. No significant differences between generations were apparent for *He* ($He_{\text{silver eels}} = 0.744$, $He_{\text{glass eels}} = 0.743$, $p = 0.54$), *Ar* ($Ar_{\text{silver eels}} = 11.74$, $Ar_{\text{glass eels}} = 11.83$, $p = 0.46$) and F_{IS} ($F_{IS\ \text{silver eels}} = 0.165$, $F_{IS\ \text{glass eels}} = 0.162$, $p = 0.07$). *Ho*, however, was significantly higher in the “*silver eel*” group ($Ho_{\text{silver eels}} = 0.621$, $Ho_{\text{glass eels}} = 0.612$, $p<0.01$). The AMOVA between “*silver eel*” and “*glass eel*” groups of

replicates revealed a pattern of isolation by time (F_{CT} = 0.002, p<0.001), supporting our a-priori assumption that those groups represent clear age structured cohorts.

None of the replicates showed evidence of heterozygote excess or deficiency. Averaged allele frequencies of neither "*silver eels*" nor "*glass eels*" deviated from an expected L-shape distribution (Fig. S3). However, we found that the averaged allele frequencies distribution observed in the "*silver eels*" group showed the signature of a 5-generations-old bottleneck identified from computer simulations (Luikart et al. 1998). This is particularly evident in the distribution of the two most common allele classes, 0.8-0.9 and 0.9-1.0. This signature was not visible anymore in the "*glass eel*" group (Fig. S4).

Estimates of effective population size (N_e) amongst replicates ranged between 0 - 625.2 for "*silver eels*" and 0 - 2708.9 for "*glass eels*". The harmonic mean of effective population size estimates amongst replicates, $\hat{N}_e$, resulted in 480.9 < $\hat{N}_{e\ \text{silver eels}}$ <2941.7 and 1380.2< $\hat{N}_{e\ \text{glass eels}}$ < 3506.0 (Table S2).

Adaptive marker: the MHC

Molecular indices and population structure

We sequenced a 247 bp fragment of the exon 2 of the MHC class II region (91% of the total size of the exon) in 327 individuals using 454 sequencing technology. We detected 229 different amino acid coding variants. Among those, 226 (98%) were found to be unique in the dataset but present in both independent replicated reactions and therefore kept as true variants (Data S3). A total of 116.276 sequence reads were used in this study. Amongst locations, MHC

363 nucleotide diversity ranged between 0.102 (LL) and 0.138 (BT). The mean number of alleles per
364 individual ranged between 2 (Q, SE = 0.298) and 4 (G_BU, SE = 0.392) (Table S3) and revealed to
365 overall significantly differ amongst sampled locations (F_{17} = 1.674, p = 0.046). However, post-
366 hoc pairwise comparisons showed no significant differences between pairs of populations after
367 correction for multiple testing (all p>0.05). The mean nucleotide divergence (p-distance) ranged
368 between 0.078 (BL) and 0.141 (FI) (Table S4) and was significantly different among sampled
369 locations (F_{17} = 1.860, p = 0.021). Post-hoc pairwise comparisons revealed two significant
370 comparisons after correction for multiple testing (GER *vs* FI, t = -3.551, p =0.045, GER *vs*
371 G_AD2011, t = -3.961, p =0.010), suggesting a reduced MHC diversity the stocked freshwater
372 system of the Schwentine river, in Germany.

373 The ANOSIM showed no significant differences in MHC allele pools amongst populations
374 (R=0.001, p = 0.98). Overall, no correlation was found between Bray-Curtis similarity matrices
375 on MHC and pairwise F_{ST} for both mtDNA (R^2 <0.0001, p =0.58) and microsatellites (R^2 <0.0001,
376 p =0.62).

377 Between generations, no difference in MHC allele pools were observed (R=-0.011, p=0.87).
378 Interestingly, "*glass eels*" had a significantly higher individual mean number of alleles ("*glass*
379 *eels*"= 3.423, SE = 0.166; "*silver eels* "= 2.856, SE = 0.101; F_1 = 8.819, p = 0.003) and a
380 significantly higher individual mean nucleotide p-distance ("*glass eels*" = 0.117, SE = 0.006;
381 "*silver eels*" = 0.101, SE =0.004; F_1= 4.577, p = 0.032) (Table 3). Both the nucleotide diversity (π)
382 and the number of minimum recombination events (*Rm*) detected between "*silver eels*" and

383 "*glass eels*" were similar ($\pi_{\text{glass eels}} = 0.118$, $\pi_{\text{silver eels}} = 0.123$; $Rm_{\text{silver eels}} = 11$; $Rm_{\text{glass eels}} = 10$)

384 while the R/θ ratio was slightly higher in "*silver eels*" ($R/\theta_{\text{silver eels}} = 2.174$; $R/\theta_{\text{glass eels}} = 2.089$).

Screening for novel genetic diversity through events of gene conversion

Gene conversion segments with an average nucleotide length of 4 bp were detected within the "*glass eels*" group but not in the "*silver eel*" group. The average ψ of the whole segment was found to be 0.0002 (Fig. 3). This value is high enough to ascertain the occurrence of conversion events, but not robust enough to determine the exact length of the observed tracts (Betran et al. 1997).

Testing for positive selection

Model-based tests using CODEML revealed 11 sites under positive selection while MEME identified 27 sites that have experienced episodic events of positive selection (Table S6). The discrepancies between the two methods reflect the different assumptions underlying the fixed effect models implemented in CODEML and the mixed effect models of MEME. Positively selected sites detected by both methods matched 10 out of 19 antigen binding sites identified in humans by X-ray crystallography (Reche & Reinherz 2003) (Fig. 3, Text S1). Due to the functional role of the MHC, all amino acid sites that have experienced at least episodic events of selection were selected for further analyses (Fig. 3)

Demography and historical profile of MHC genetic diversity

All mismatch distributions indicated a clear deviation from a constant population size, fitting a scenario where a major demographic event occurred (Fig. 4 and Fig. 5). The frequency distribution of pairwise differences showed different peaks for both PSS (Fig. 4) and nPSS (PSS $_{\text{pairwise differences}}$ = 20; nPSS $_{\text{pairwise differences}}$ =10) (Fig. 5). Those peaks reflect old lineages that are maintained in genes exhibiting trans-species polymorphism as is expected of the MHC (Klein et

406 al. 2007) and recently reported for the European eel (Bracamonte et al. 2015). It was also
407 possible to observe peaks in PSS and nPSS in the frequency of pairwise differences equaling 1.
408 Those peaks are suggestive of increases in genetic diversity. No differences in the demographic
409 profiles were detected between "*silver eels*" and "*glass eels*" (Fig. 4 and Fig. 5).

410 Bayesian demographic reconstructions revealed a steep decline in genetic diversity that
411 occurred close to the present time. This pattern is characteristic of a genetic bottleneck and is
412 shared by all reconstructions independently of the substitution rates (Fig. 4). However, lineage-
413 through-time plots reveal a very recent burst of lineage diversification, also at t=0 and common
414 to both generations (Fig. 6). The three independent MCMC runs clearly overlap for the
415 distributions of the posterior, likelihood and skyline estimates (Fig. S5), assuring that the
416 profiles observed were not a product of the Bayesian stochasticity, but rather a real and
417 reproducible pattern.

418 Discussion

419 We investigated how the steep decline in European eel recruitment observed in the 1980s and
420 subsequent population reduction may have affected this species' genetic diversity. We
421 expanded on previous studies (Pujolar et al. 2011; Pujolar et al. 2013; Wirth & Bernatchez 2003)
422 and searched for contemporary signature of a population reduction by considering neutral
423 markers (mtDNA or microsatellites) as well as a highly polymorphic region of the immune genes
424 of the MHC. Although MHC is an excellent marker to evaluate genetic diversity, as a proxy for
425 adaptive potential, in endangered populations (Sommer 2005; Sutton et al. 2015), no formal
426 study of its variation and evolution exist for the European eel.

Location-specific patterns of genetic diversity and demographic estimates

Although it was not the primary focus of this study, spatial comparison of mtDNA genetic diversity provided information on the genetic differentiation amongst continental locations. Under neutrality, haplotype and nucleotide diversities are predicted to be a function of population size (Frankham et al. 2002). Therefore, in the drastically declined European eel population, we expected to find an overall low genetic diversity. Furthermore, and due to reports of panmixia (Als et al. 2011), we also expected coherent patterns amongst sampled locations. Instead, we found variation in nucleotide diversity (0.003-0.008), haplotype diversity (0.575-0.934) and Tajima´s *D* estimates amongst locations. The high variation in genetic indices amongst geographical areas suggests that processes act differently across the continental distribution of the European eel. Our observations may result from the post-hatching transatlantic migration, since simulations showed variability in spawning grounds would leave genetic signatures across continental locations under low recruitment (Baltazar-Soares et al. 2014). Conversely, it could be explained by a scenario where mtDNA haplotypes are linked to genes under single-generation local selection (Pujolar et al. 2014). In this scenario, selection would act mainly in the local foraging environment, and not in the spawning ground, with specific pressures sorting out genotypes in given locations. Expanding the study towards a more genomic approach with adult fish sampled from the spawning ground would reveal further insights into the most prominent scenario.

Due to high levels of polymorphism, neutrally evolving microsatellites are thought to be sensitive enough to detect subtle shifts in population dynamics (England et al. 2010). Here as well, we hypothesized that the chronically low recruitment in European eel observed since the 1980s had negatively affected estimates of genetic diversity in a coherent spatial pattern. Estimates of allelic richness (*Ar* = 2.710-2.960) and heterozygosity estimates (*He* = 0.687-0.758) were very similar, and neither mode shifts nor heterozygote excesses were observed (Fig. 1 and Fig. S1). These results are in line with a previous study (Pujolar et al. 2011), which was conducted focusing on 12 locations (3 locations sampled across a temporal range) and that employed 22 EST-linked microsatellites. The apparent homogeneity of the allelic indices amongst locations matches the expectations based on neutral nuclear markers for a panmictic population where successfully recruited mature fish would mate randomly in the spawning ground (Als et al. 2011). Note, after correction for multiple testing, we detected significantly different pairwise F_{ST} estimates amongst some locations. Although this could suggest deviations from panmixia, it is likely this pattern is linked to stochasticity due to low sample sizes in those locations (G_NIRL, G_TITA and G_WENG).

Regarding the MHC, we found differences in the mean number of alleles amongst locations although none of the post-hoc pairwise comparisons revealed to be significant after correction for multiple testing. MHC allele pool composition did not vary amongst sampled locations. We found that the mean nucleotide distances vary amongst locations, but only comparisons between the German populations and two other sampled locations revealed to be significant after correction for multiple testing (Germany *vs* Finland, Germany *vs* France2011). Whether it relates to the fact that those samples correspond to a freshwater system, the Schwentine in

Germany, where all eels are stocked remains to be investigated. Stocking however might be an issue in other sampling areas as well and therefore understanding why this population demonstrates a reduction in diversity should be the focus of further studies.

Genetic diversity and demographic estimates between age cohorts

Recruitment decline of the 1980s did not affected genetic estimates of neutral evolving markers

The major objective of this study was to compare patterns of temporal variation of genetic diversity post-recruitment collapse observed in the 1980s. Here as well, our mitochondrial DNA results showed i) no evidence for a genetic bottleneck, ii) no differences in haplotype and nucleotide diversities between "*silver eels*" and "*glass eels*", and iii) no signature of bottleneck in the frequency distribution of pairwise mismatches. The later rather points towards an historical population expansion (Rogers & Harpending 1992). Given the low variability of the mtDNA marker – in comparison with the set of highly polymorphic microsatellites and MHC gene – we suggest that such an event extends back in time to a scenario of expansion related to ice-sheet retreat after the last glacial maxima, as previously proposed for such a pattern (Jacobsen et al. 2014).

Investigating the distribution of the genetic variance observed at microsatellites, we found significant differentiation between "*silver eels*" and "*glass eels*" replicates. This pattern of genetic variance distribution is in line with previous reports that also attributed higher genetic

489 variance amongst temporal, rather than spatial, partitions of *A. anguilla* along the European
490 coasts (Dannewitz et al. 2005). It also confirmed our a-priori assumption of each group
491 representing a distinct generation, and therefore excludes possible confounding factors
492 associated with overlapping generations from the interpretation of demographic estimates
493 (Cornuet & Luikart 1996; Waples & Do 2010). Note, even though less likely, we cannot exclude
494 that this observed structure also relates to a spatially structured spawning area of this species
495 (Baltazar-Soares et al. 2014; Dannewitz et al. 2005).

496 Using microsatellites, we detected no evidence of heterozygote excess in any of the replicates,
497 nor any differences between allelic richness of "*silver eels*" and "*glass eels*". This supports
498 previous reports that the recruitment collapse and subsequent low abundance of the eel
499 population did not leave the expected genetic signatures of reduced genetic diversity (Pujolar
500 et al. 2011) suggestive of a system which replenishes genetic diversity rapidly.

501 However, in-depth demographic analyses suggest that the eel effective population size might
502 actually not be stable. Several lines of evidence support this interpretation: firstly, we
503 estimated ~20% higher effective population size in "*glass eel*" replicates (harmonic mean
504 N_e=3506.0) compared to "*silver eels*" (N_e = 2941.7). These contemporary estimates are near the
505 lower confidence intervals of historic effective population sizes previously reported (5000 < N_e
506 <10000; (Wirth & Bernatchez 2003), but within contemporary estimates of 3000 < N_e <12000
507 (Pujolar et al. 2011)). Noteworthy, the confidence intervals calculated in this study for each
508 generation overlap, raising the need to cautiously interpret those results. Secondly, we
509 observed fewer alleles in the most frequent class of allele frequencies in "*silver eels*". The

apparent reduction of the most frequent allele class may suggest that the species demography is experiencing a transitory stage from a severe bottleneck, partly detected in "*silver eels*". It is important to mention that such a signature would only be detected under a severe population reduction a few generations in the past. Hence, we could speculate that the hypothetical bottleneck detected only in "*silver eels*" may relate to the drops in European eel recruitment that occurred in the beginning of the 1960s (EIFAAC/ICES 2011). It is possible that the 1960s low recruitment had a major impact on the overall genetic diversity of the species. By the crash in the 1980s, the population would have already been depleted from its original genetic diversity, at least for neutrally evolving markers. Such a scenario requires further studies to be confirmed and would rely on historical samples to be analyzed.

MHC reveals signatures of selection

Extending the evaluation of genetic diversity to the evolutionary analysis of the adaptive immune genes of the MHC was motivated by two main reasons. The first relates to studies suggesting MHC diversity to be more sensitive than neutrally evolving markers in the detection of demographic shifts (Sommer 2005; Sutton et al. 2011). The second relates to the invasion of European freshwater systems by the nematode parasite, *Anguillicola crassus,* for which the MHC was found to respond to in the paratenic host, the three-spined stickleback (Eizaguirre et al. 2012b). Using the exon 2 of the MHC class II β gene, we evaluated 1) genetic diversity, which might have been affected by the recruitment collapse and subsequent population reduction and 2) allele frequency shifts between generations which would be a signature consistent with directional parasite-mediated selection.

Using next-generation sequencing, we identified a total of 229 MHC alleles amongst 327 individuals. This indicates that the diversity within this species is not low and directly compares to observations made in wild populations of other fishes that are not qualified as endangered, such as for instances, the half-smooth tongue sole (88 MHC class II alleles amongst 160 individuals) (Du et al. 2011). Noteworthy, the characterization of the MHC class II genes in this species revealed that up to six different alleles may exist per individual, suggesting the presence of at least three loci (Bracamonte et al. 2015; Bracamonte 2013). Because next generation sequencing is thought to generally overestimate the number of MHC alleles detected (Babik et al. 2009; Lighten et al. 2014; Sommer et al. 2013), we took multiple precautions to avoid artifacts (reconditioning steps, reduced numbers of PCR cycles, duplicates). Despite such precautions and sequence confirmation using cloning (performed in (Bracamonte et al. 2015)), we cannot exclude that some variants were called alleles even though artifactual (Sommer et al. 2013). Again, as mtDNA sequencing revealed a large number of haplotypes (N=102), the large diversity at the MHC displayed in this species may not be surprising.

Generally, our results are suggestive of a pattern of selective sweep at the MHC between the two generations examined here. We found *"silver eels"* to exhibit lower mean number of alleles and lower mean nucleotide distance than "*glass eels*", suggesting that the "*silver eel*" generation was under a selective pressure that reduced its pool of MHC alleles to fewer and more similar alleles. This observation suggests that either the selective pressure was widespread amongst continental locations or that it acted when all eels experienced similar conditions, as for instance, during the fastening spawning migration. A hypothetical selective pressure imposed by *A. crassus* meets both criteria. Not only is this parasite ubiquitous in

European freshwater systems (Wielgoss et al. 2008a) but it also impairs the swimming performance of infected eels (Palstra et al. 2007).

Overall, the higher genetic diversity of "*glass eels*" together with the identification of two short gene conversions in this study suggest an ongoing regeneration of the species immune adaptive potential. Indeed gene conversation is a mechanism capable of generating novel diversity within the MHC region, and seems to be a predominant mechanism in genetically depauperate populations (Spurgin et al. 2011).

Contemporary loss of MHC diversity: evidence of selection?

The parasite *A. crassus* was presumably introduced in the European freshwater systems at the beginning of the 1980s (Taraschewski et al. 1987), quickly spreading across continental water bodies. The European eel is particularly susceptible to *A. crassus* infection (Knopf 2006) and therefore its introduction provides an excellent biological calibration to evaluate its impact on the evolution of diversity of the MHC. More specifically, we expected a signature of selection by the parasite to be reflected in positively selected sites of the MHC variants. In total, we detected 27 sites to be under or that have experienced positive selection along their evolutionary history.

Bayesian skyline plots showed a steep decline in MHC genetic diversity as time approaches present. This pattern is visible independently of the substitution rates and is reproducible with independent runs, i.e. overlap of the probability density distributions of the posterior, skyline and likelihood. Together, this suggests a real pattern and not an artifact. This decline in genetic diversity of the adaptive gene is similar to those detected in genealogies exposed to events of

574 episodic positive selection (Bedford et al. 2011), but also in functional regions involved in
575 adaptive responses (Padhi & Verghese 2008). Two main factors may explain it. Firstly, it can be
576 attributed to the long terminal branching typical of phylogenies of genes evolving under
577 balancing selection (Richman 2000), amongst which the MHC is a classic example (Klein et al.
578 2007). MHC class II genes are also classical examples of genes evolving through recombination
579 (Reusch & Langefors 2005) and gene conversion (Spurgin et al. 2011) – two mechanisms that
580 together with a relatively high copy number variation generates rapid genetic novelty (Chain et
581 al. 2014). Therefore, a null expectation for balancing selection and generation of rapid genetic
582 diversity – as predicted for MHC - would rather be that of either an expanding or stable
583 population, which was not what we observed here.

584 Conversely, it can be attributed to an event of selection speculatively associated with the
585 spread of *A. crassus* across the European freshwater systems. *A. crassus* was unknown to *A.*
586 *anguilla* before its recent introduction, however it is naturally present in the *A. japonica*
587 population (Wielgoss et al. 2008a). Hence, the frequency of the MHC alleles, or group of
588 functionally similar MHC alleles, that confer resistance against this parasite would either be low
589 or even absent in the European eel population (Eizaguirre et al. 2012b). The selection for those
590 rare variants could have triggered the major loss of diversity we observed in the Bayesian plots
591 and confirmed by the lower diversity indices of the "*silver eels*". Interestingly, the allelic lineage
592 diversity of the MHC showed a constant increase with a particular acceleration approaching the
593 contemporary period, as indicated by the lineages-through-time-plots of both generations.
594 While we are unable to provide a direct functional link between such diversification and our
595 observations of gene conversion and recombination within this specific MHC region, these

596 mechanisms have been associated with signatures of recovery after a genetic bottleneck in
597 genes under balancing selection (Richman 2000). Therefore, the inferred recent steep decline
598 followed by a very recent burst of lineage diversification upholds the occurrence of a selective
599 sweep in the MHC genealogy that pre-dated both our sampling points, as suggested by the
600 comparison between "*silver eels*" and "*glass eels*", with an ongoing recovery of the MHC
601 diversity.

602 From our results we can hypothesize two scenarios. A first scenario involves a link between a
603 sudden reduction in population size, a loss of genetic diversity and a constant selective pressure
604 extending after the bottleneck. In this scenario, genetic drift would affect overall genetic
605 diversity but since selection would continue to act, genetic diversity of positively selected
606 regions would remain low (Eimes et al. 2011). A second scenario relates to multiple MHC loci
607 carrying similar alleles due to recent duplications and to the hypothesis that a population would
608 experience a size reduction and an event of selection within the same time frame. In this
609 scenario, the selective pressure through the bottleneck would lead to a faster fixation of
610 resistant alleles (Eimes et al. 2011).

611 **Limits of the study**

612 Evaluating demography in the European eel is complex particularly due to the difficulty of
613 sampling them at their mating ground and the reliance on indirect genetic evidence. Even
614 though patterns of selection and recent recovery of the MHC diversity seem robust, due to the
615 high allelic variation reported in this gene, we acknowledge that other coalescence models
616 could revealed refined patterns (Árnason & Halldórsdóttir 2015; Wakeley 2013). It is indeed

possible that multiple loci analysed together as one locus – although with same functional basis - could create a pattern similar to multiple coalescence. To the best of our knowledge, multiple merger models such as those described by Árnason and Halldórsdóttir (Árnason & Halldórsdóttir 2015) have not yet been applied to investigate the evolutionary signature that linked copies of the same (functional) gene produce on the evaluation of genetic diversity and demography. This thus limits working hypotheses and would be difficult to interpret. Nonetheless, while further investigations are obviously needed to clarify fluctuations in genetic diversity in such a complex but evolutionary relevant immune gene, we argue that our work represents a first empirical step along this line of research.

Conclusions

In summary, our work reveals signatures of recent reduction in MHC genetic diversity and suggests signs of ongoing recovery of this gene's diversity contributing to the immunogenetic adaptive potential of this endangered species (Radwan et al. 2010; Sommer 2005; Stiebens et al. 2013b). Future research will be needed to provide conclusive evidence as to which scenario holds, accommodating also newer theories to further verify the validity of our findings. A future perspective would be to extend the time-series analyses by incorporating screening of MHC diversity in ongoing monitoring practices. This would be a valuable approach to access the evolution of the species adaptive potential.

636 ## Acknowledgments

637 The authors wish to thank J. Duhart, K. Bodles, D. Evans, E. Prigge and L. Marohn for eel
638 samples; J. Klein, L. Listmann, J. Nickel and M. Hoffmann for assistance with laboratory work; M.
639 Heckwolf and P. Roedler for help in processing glass eel samples; R. Scott for help designing the
640 maps.

641

642

643

644

645

646

647

648

649 ## References

650 Allendorf FW, England PR, Luikart G, Ritchie PA, and Ryman N. 2008. Genetic effects of harvest on wild
651 animal populations. *Trends in Ecology & Evolution* 23:327-337.
652 Als TD, Hansen MM, Maes GE, Castonguay M, Riemann L, Aarestrup K, Munk P, Sparholt H, Hanel R, and
653 Bernatchez L. 2011. All roads lead to home: panmixia of European eel in the Sargasso Sea.
654 *Molecular Ecology* 20:1333-1346.
655 Apanius V, Penn D, Slev PR, Ruff LR, and Potts WK. 1997. The nature of selection on the major
656 histocompatibility complex. *Critical Reviews in Immunology* 17.
657 Árnason E, and Halldórsdóttir K. 2015. Nucleotide variation and balancing selection at the Ckma gene in
658 Atlantic cod: analysis with multiple merger coalescent models. *PeerJ* 3:e786.
659 Babik W, Taberlet P, Ejsmond MJ, and Radwan J. 2009. New generation sequencers as a tool for
660 genotyping of highly polymorphic multilocus MHC system. *Molecular Ecology Resources* 9:713-
661 719.
662 Baltazar-Soares M, Biastoch A, Harrod C, Hanel R, Marohn L, Prigge E, Evans D, Bodles K, Behrens E,
663 Böning Claus W, and Eizaguirre C. 2014. Recruitment Collapse and Population Structure of the
664 European Eel Shaped by Local Ocean Current Dynamics. *Current biology : CB* 24:104-108.
665 Bedford T, Cobey S, and Pascual M. 2011. Strength and tempo of selection revealed in viral gene
666 genealogies. *BMC evolutionary biology* 11:220.
667 Belkir K BP, Goudet J, Chikhi L, Bonhomme F. 1999. Genetix, logiciel sous Windows TM pour la genetique
668 des populations. In: Laboratoire Genome et Populations UdM, editor. France.
669 Betran E, Rozas J, Navarro A, and Barbadilla A. 1997. The estimation of the number and the length
670 distribution of gene conversion tracts from population DNA sequence data. *Genetics* 146:89-99.
671 Bonhommeau S, Chassot E, and Rivot E. 2008. Fluctuations in European eel (Anguilla anguilla)
672 recruitment resulting from environmental changes in the Sargasso Sea. *Fisheries Oceanography*
673 17:32-44.
674 Bracamonte S, Baltazar-Soares M, and Eizaguirre C. 2015. Characterization of MHC class II genes in the
675 critically endangered European eel (Anguilla anguilla). *Conservation Genetics Resources*:1-12.
676 Bracamonte SE. 2013. Characterization and evolution of MHC II genes in the European eel (Anguilla
677 anguilla). Christian-Albrechts-Universität Kiel.
678 Chain FJ, Feulner PG, Panchal M, Eizaguirre C, Samonte IE, Kalbe M, Lenz TL, Stoll M, Bornberg-Bauer E,
679 and Milinski M. 2014. Extensive copy-number variation of young genes across stickleback
680 populations. *PLoS genetics* 10:e1004830.
681 Clarke KR. 1993. Non-parametric multivariate analyses of changes in community structure. *Australian*
682 *Journal of Ecology*:117-143.
683 Cornuet JM, and Luikart G. 1996. Description and power analysis of two tests for detecting recent
684 population bottlenecks from allele frequency data. *Genetics* 144:2001-2014.
685 Dannewitz J, Maes GE, Johansson L, Wickström H, Volckaert FAM, and Järvi T. 2005. Panmixia in the
686 European eel: a matter of time. *Proceedings of the Royal Society B: Biological Sciences* 272:1129-
687 1137.
688 Darriba D, Taboada GL, Doallo R, and Posada D. 2012. jModelTest 2: more models, new heuristics and
689 parallel computing. *Nature Methods* 9:772-772.
690 Dekker W. 2003. Did lack of spawners cause the collapse of the European eel, Anguilla anguilla? *Fisheries*
691 *Management and Ecology* 10:365-376.
692 Delport W, Poon AF, Frost SD, and Pond SLK. 2010. Datamonkey 2010: a suite of phylogenetic analysis
693 tools for evolutionary biology. *Bioinformatics* 26:2455-2457.
694 Do C, Waples RS, Peel D, Macbeth G, Tillett BJ, and Ovenden JR. 2014. NeEstimator v2: re-
695 implementation of software for the estimation of contemporary effective population size (Ne)
696 from genetic data. *Molecular Ecology Resources* 14:209-214.

697 Drummond AJ, and Rambaut A. 2007. BEAST: Bayesian evolutionary analysis by sampling trees. *BMC*
698 *evolutionary biology* 7:214.
699 Drummond AJ, Rambaut A, Shapiro B, and Pybus OG. 2005. Bayesian coalescent inference of past
700 population dynamics from molecular sequences. *Molecular Biology and Evolution* 22:1185-1192.
701 Du M, Chen S-l, Liu Y-h, Liu Y, and Yang J-f. 2011. MHC polymorphism and disease resistance to vibrio
702 anguillarum in 8 families of half-smooth tongue sole (Cynoglossus semilaevis). *BMC Genetics*
703 12:78.
704 EIFAAC/ICES. 2011. Country reports WGEEL 2011. Report on the eel stock and fisheries.
705 EIFAAC/ICES. 2013. Country reports WGEEL 2013. Report on the eel stock and fisheries.
706 Eimes J, Bollmer J, Whittingham L, Johnson J, Van Oosterhout C, and Dunn P. 2011. Rapid loss of MHC
707 class II variation in a bottlenecked population is explained by drift and loss of copy number
708 variation. *Journal of Evolutionary Biology* 24:1847-1856.
709 Eizaguirre C, and Baltazar-Soares M. 2014. Evolutionary Conservation-Evaluating the adaptive potential
710 of species. *Evolutionary Applications*.
711 Eizaguirre C, Lenz TL, Kalbe M, and Milinski M. 2012a. Divergent selection on locally adapted major
712 histocompatibility complex immune genes experimentally proven in the field. *Ecology Letters*
713 15:723-731.
714 Eizaguirre C, Lenz TL, Kalbe M, and Milinski M. 2012b. Rapid and adaptive evolution of MHC genes under
715 parasite selection in experimental vertebrate populations. *Nat Commun* 3:621.
716 Eizaguirre C, Lenz TL, Sommerfeld RD, Harrod C, Kalbe M, and Milinski M. 2011. Parasite diversity,
717 patterns of MHC II variation and olfactory based mate choice in diverging three-spined
718 stickleback ecotypes. *Evolutionary Ecology* 25:605-622.
719 England PR, Luikart G, and Waples RS. 2010. Early detection of population fragmentation using linkage
720 disequilibrium estimation of effective population size. *Conservation genetics* 11:2425-2430.
721 Excoffier L, and Lischer HEL. 2009. Arlequin suite ver 3.5: a new series of programs to perform
722 population genetics analyses under Linux and Windows. *Molecular Ecology Resources* 10:564-
723 567.
724 Frankham R, Briscoe DA, and Ballou JD. 2002. *Introduction to conservation genetics*: Cambridge
725 University Press.
726 Friedland KD, Miller MJ, and Knights B. 2007. Oceanic changes in the Sargasso Sea and declines in
727 recruitment of the European eel. *ICES Journal of Marine Science: Journal du Conseil* 64:519-530.
728 Goudet J. 1995. FSTAT (version 1.2): a computer program to calculate F-statistics. *Journal of Heredity*
729 86:485-486.
730 Guindon S, and Gascuel O. 2003. A simple, fast, and accurate algorithm to estimate large phylogenies by
731 maximum likelihood. *Systematic biology* 52:696-704.
732 Harrod C, Grey J, McCarthy T, and Morrissey M. 2005. Stable isotope analyses provide new insights into
733 ecological plasticity in a mixohaline population of European eel. *Oecologia* 144:673-683.
734 Hendry AP, Kinnison MT, Heino M, Day T, Smith TB, Fitt G, Bergstrom CT, Oakeshott J, Jørgensen PS,
735 Zalucki MP, Gilchrist G, Southerton S, Sih A, Strauss S, Denison RF, and Carroll SP. 2011.
736 Evolutionary principles and their practical application. *Evolutionary Applications* 4:159-183.
737 Hood GM. 2010. PopTools version 3.2.5 Available on the internet.
738 Hudson RR, and Kaplan NL. 1985. Statistical properties of the number of recombination events in the
739 history of a sample of DNA sequences. *Genetics* 111:147-164.
740 ICES. 2015. ICES WKEELCITES REPORT 2015. Report on the eel stock and fisheries.
741 Jacobsen M, Pujolar JM, Gilbert MTP, Moreno-Mayar J, Bernatchez L, Als TD, Lobon-Cervia J, and Hansen
742 MM. 2014. Speciation and demographic history of Atlantic eels (Anguilla anguilla and A.
743 rostrata) revealed by mitogenome sequencing. *Heredity* 113:432-442.

744 Janeway CA, Travers P, Walport M, and Shlomchik MJ. 2005. Immunobiology: the immune system in
745 health and disease.
746 Kalinowski ST. 2005. hp-rare 1.0: a computer program for performing rarefaction on measures of allelic
747 richness. *Molecular Ecology Notes* 5:187-189.
748 Keith DA, Akçakaya HR, Thuiller W, Midgley GF, Pearson RG, Phillips SJ, Regan HM, Araujo MB, and
749 Rebelo TG. 2008. Predicting extinction risks under climate change: coupling stochastic
750 population models with dynamic bioclimatic habitat models. *Biology Letters* 4:560-563.
751 Kettle AJ, Bakker DCE, and Haines K. 2008a. Impact of the North Atlantic Oscillation on the trans-Atlantic
752 migrations of the European eel (Anguilla anguilla). *J Geophys Res* 113:G03004.
753 Kettle AJ, Bakker DCE, and Haines K. 2008b. Impact of the North Atlantic Oscillation on the trans-Atlantic
754 migrations of the European eel (Anguilla anguilla). *Journal of Geophysical Research-*
755 *Biogeosciences* 113:26.
756 Kimura M, and Ohta T. 1978. Stepwise mutation model and distribution of allelic frequencies in a finite
757 population. *Proceedings of the National Academy of Sciences* 75:2868-2872.
758 Kingman JFC. 1982. The coalescent. *Stochastic processes and their applications* 13:235-248.
759 Kirk RS. 2003. The impact of Anguillicola crassus on European eels. *Fisheries Management and Ecology*
760 10:385-394.
761 Klein J, Sato A, and Nikolaidis N. 2007. MHC, TSP, and the origin of species: from immunogenetics to
762 evolutionary genetics. *Annu Rev Genet* 41:281-304.
763 Knopf K. 2006. The swimbladder nematode Anguillicola crassus in the European eel Anguilla anguilla and
764 the Japanese eel Anguilla japonica: differences in susceptibility and immunity between a
765 recently colonized host and the original host. *Journal of Helminthology* 80:129-136.
766 Lenz TL, and Becker S. 2008. Simple approach to reduce PCR artefact formation leads to reliable
767 genotyping of *MHC* and other highly polymorphic loci. Implications for evolutionary analysis.
768 *Gene* 427:117-123.
769 Lenz TL, Eizaguirre C, Kalbe M, and Milinski M. 2013. Evaluating patterns of convergent evolution and
770 trans-species polymorphism at MHC immunogenes in two sympatric stickleback species
771 *Evolution* 67:2400-2412.
772 Librado P, and Rozas J. 2009. DnaSP v5: a software for comprehensive analysis of DNA polymorphism
773 data. *Bioinformatics* 25:1451-1452.
774 Lighten J, Oosterhout C, and Bentzen P. 2014. Critical review of NGS analyses for de novo genotyping
775 multigene families. *Molecular Ecology*.
776 Luikart G, Allendorf F, Cornuet J, and Sherwin W. 1998. Distortion of allele frequency distributions
777 provides a test for recent population bottlenecks. *Journal of Heredity* 89:238-247.
778 Maes G, and Volckaert F. 2002. Clinal genetic variation and isolation by distance in the European eel
779 Anguilla anguilla (L.). *Biological Journal of the Linnean Society* 77:509-521.
780 McCallum H. 2008. Tasmanian devil facial tumour disease: lessons for conservation biology. *Trends in*
781 *Ecology & Evolution* 23:631-637.
782 McMahon BJ, Teeling EC, and Höglund J. 2014. How and why should we implement genomics into
783 conservation? *Evolutionary Applications*.
784 Miller MJ. 2009. Ecology of anguilliform leptocephali: remarkable transparent fish larvae of the ocean
785 surface layer. *Aqua-BioSci Monogr* 2.
786 Munk P, Hansen MM, Maes GE, Nielsen TG, Castonguay M, Riemann L, Sparholt H, Als TD, Aarestrup K,
787 Andersen NG, and Bachler M. 2010. Oceanic fronts in the Sargasso Sea control the early life and
788 drift of Atlantic eels. *Proceedings of the Royal Society B: Biological Sciences* 277:3593-3599.
789 Murrell B, Wertheim JO, Moola S, Weighill T, Scheffler K, and Kosakovsky Pond SL. 2012. Detecting
790 Individual Sites Subject to Episodic Diversifying Selection. *PLoS Genet* 8:e1002764.

791 Narum SR. 2006. Beyond Bonferroni: less conservative analyses for conservation genetics. *Conservation*
792 *genetics* 7:783-787.
793 Nee S, Mooers AO, and Harvey PH. 1992. Tempo and mode of evolution revealed from molecular
794 phylogenies. *Proceedings of the National Academy of Sciences* 89:8322-8326.
795 Padhi A, and Verghese B. 2008. Positive natural selection in the evolution of human metapneumovirus
796 attachment glycoprotein. *Virus research* 131:121-131.
797 Palstra AP, Heppener DFM, van Ginneken VJT, Székely C, and van den Thillart GEEJM. 2007. Swimming
798 performance of silver eels is severely impaired by the swim-bladder parasite Anguillicola
799 crassus. *Journal of Experimental Marine Biology and Ecology* 352:244-256.
800 Piertney S, and Oliver M. 2006. The evolutionary ecology of the major histocompatibility complex.
801 *Heredity* 96:7-21.
802 Pond SLK, and Frost SD. 2005. Datamonkey: rapid detection of selective pressure on individual sites of
803 codon alignments. *Bioinformatics* 21:2531-2533.
804 Prigge E, Marohn L, Oeberst R, and Hanel R. 2013. Model prediction vs. reality—testing the predictions
805 of a European eel (Anguilla anguilla) stock dynamics model against the in situ observation of
806 silver eel escapement in compliance with the European eel regulation. *ICES Journal of Marine*
807 *Science: Journal du Conseil* 70:309-318.
808 Pritchard JK, Stephens M, and Donnelly P. 2000. Inference of population structure using multilocus
809 genotype data. *Genetics* 155:945-959.
810 Pujolar J, Bevacqua D, Capoccioni F, Ciccotti E, De Leo G, and Zane L. 2011. No apparent genetic
811 bottleneck in the demographically declining European eel using molecular genetics and forward-
812 time simulations. *Conservation genetics* 12:813-825.
813 Pujolar JM, Jacobsen M, Als TD, Frydenberg J, Munch K, Jonsson B, Jian JB, Cheng L, Maes GE, and
814 Bernatchez L. 2014. Genome-wide single-generation signatures of local selection in the
815 panmictic European eel. *Molecular Ecology* 23:2514-2528.
816 Pujolar JM, Jacobsen M, Frydenberg J, Als TD, Larsen PF, Maes G, Zane L, Jian J, Cheng L, and Hansen
817 MM. 2013. A resource of genome-wide single-nucleotide polymorphisms generated by RAD tag
818 sequencing in the critically endangered European eel. *Molecular Ecology Resources* 13:706-714.
819 Pujolar JM, Maes GE, Van Houdt JKJ, and Zane L. 2009. Isolation and characterization of expressed
820 sequence tag-linked microsatellite loci for the European eel (Anguilla anguilla). *Molecular*
821 *Ecology Resources* 9:233-235.
822 Radwan J, Biedrzycka A, and Babik W. 2010. Does reduced MHC diversity decrease viability of vertebrate
823 populations? *Biological Conservation* 143:537-544.
824 Reche PA, and Reinherz EL. 2003. Sequence variability analysis of human class I and class II MHC
825 molecules: functional and structural correlates of amino acid polymorphisms. *Journal of*
826 *molecular biology* 331:623-641.
827 Reusch TB, and Langefors A. 2005. Inter-and intralocus recombination drive MHC class IIB gene
828 diversification in a teleost, the three-spined stickleback Gasterosteus aculeatus. *Journal of*
829 *Molecular Evolution* 61:531-541.
830 Richman A. 2000. Evolution of balanced genetic polymorphism. *Molecular Ecology* 9:1953-1963.
831 Robinet T, and Feunteun E. 2002. Sublethal Effects of Exposure to Chemical Compounds: A Cause for the
832 Decline in Atlantic Eels? *Ecotoxicology* 11:265-277.
833 Rogers AR, and Harpending H. 1992. Population growth makes waves in the distribution of pairwise
834 genetic differences. *Molecular Biology and Evolution* 9:552-569.
835 Sommer S. 2005. The importance of immune gene variability (MHC) in evolutionary ecology and
836 conservation. *Front Zool* 2:16.

837 Sommer S, Courtiol A, and Mazzoni CJ. 2013. MHC genotyping of non-model organisms using next-
838 generation sequencing: a new methodology to deal with artefacts and allelic dropout. *BMC*
839 *genomics* 14:542.
840 Spielman D, Brook BW, and Frankham R. 2004. Most species are not driven to extinction before genetic
841 factors impact them. *Proceedings of the National Academy of Sciences of the United States of*
842 *America* 101:15261-15264.
843 Spurgin LG, and Richardson DS. 2012. How pathogens drive genetic diversity: MHC, mechanisms and
844 misunderstandings. *Proceedings of the Royal Society B: Biological Sciences* 277:979-988.
845 Spurgin LG, van Oosterhout C, Illera JC, Bridgett S, Gharbi K, Emerson BC, and Richardson DS. 2011. Gene
846 conversion rapidly generates major histocompatibility complex diversity in recently founded
847 bird populations. *Molecular Ecology* 20:5213-5225.
848 Stiebens VA, Merino SE, Chain FJ, and Eizaguirre C. 2013a. Evolution of MHC class I genes in the
849 endangered loggerhead sea turtle (Caretta caretta) revealed by 454 amplicon sequencing. *BMC*
850 *evolutionary biology* 13:95.
851 Stiebens VA, Merino SE, Roder C, Chain FJJ, Lee PLM, and Eizaguirre C. 2013b. Living on the edge: how
852 philopatry maintains adaptive potential. *Proceedings of the Royal Society B: Biological Sciences*
853 280.
854 Sutton JT, Nakagawa S, Robertson BC, and Jamieson IG. 2011. Disentangling the roles of natural
855 selection and genetic drift in shaping variation at MHC immunity genes. *Molecular Ecology*
856 20:4408-4420.
857 Sutton JT, Robertson BC, and Jamieson IG. 2015. MHC variation reflects the bottleneck histories of New
858 Zealand passerines. *Molecular Ecology* 24:362-373.
859 Tajima F. 1989. Statistical method for testing the neutral mutation hypothesis by DNA polymorphism.
860 *Genetics* 123:585-595.
861 Tamura K, Peterson D, Peterson N, Stecher G, Nei M, and Kumar S. 2011. MEGA5: molecular
862 evolutionary genetics analysis using maximum likelihood, evolutionary distance, and maximum
863 parsimony methods. *Molecular Biology and Evolution* 28:2731-2739.
864 Taraschewski H, Moravec F, Lamah T, and Anders K. 1987. Distribution and morphology of two
865 helminths recently introduced into European eel populations: Anguillicola crassus (Nematoda,
866 Dracunculoidea) and Paratenuisentis ambiguus (Acanthocephala, Tenuisentidae). *Diseases of*
867 *Aquatic Organisms* 3:167-176.
868 Tesch F. 2003. *The Eel*. Oxford: Blackwell Sciences Ltd.
869 Thomas CD, Cameron A, Green RE, Bakkenes M, Beaumont LJ, Collingham YC, Erasmus BFN, de Siqueira
870 MF, Grainger A, Hannah L, Hughes L, Huntley B, van Jaarsveld AS, Midgley GF, Miles L, Ortega-
871 Huerta MA, Townsend Peterson A, Phillips OL, and Williams SE. 2004. Extinction risk from
872 climate change. *Nature* 427:145-148.
873 Van Ginneken V, Ballieux B, Willemze R, Coldenhoff K, Lentjes E, Antonissen E, Haenen O, and van den
874 Thillart G. 2005. Hematology patterns of migrating European eels and the role of EVEX virus.
875 *Comparative Biochemistry and Physiology Part C: Toxicology & Pharmacology* 140:97-102.
876 Wakeley J. 2013. Coalescent theory has many new branches. *Theoretical Population Biology* 87:1-4.
877 Waples RS, and Do C. 2010. Linkage disequilibrium estimates of contemporary Ne using highly variable
878 genetic markers: a largely untapped resource for applied conservation and evolution.
879 *Evolutionary Applications* 3:244-262.
880 Waples RS, and Do CHI. 2008. ldne: a program for estimating effective population size from data on
881 linkage disequilibrium. *Molecular Ecology Resources* 8:753-756.
882 Weir BS. 1990. *Genetic data analysis. Methods for discrete population genetic data*: Sinauer Associates,
883 Inc. Publishers.

884 Wielgoss S, Taraschewski H, Meyer A, and Wirth T. 2008a. Population structure of the parasitic
885 nematode Anguillicola crassus, an invader of declining North Atlantic eel stocks. *Molecular*
886 *Ecology* 17:3478-3495.
887 Wielgoss S, Wirth T, and Meyer A. 2008b. Isolation and characterization of 12 dinucleotide
888 microsatellites in the European eel, Anguilla anguilla L., and tests of amplification in other
889 species of eels. *Molecular Ecology Resources* 8:1382-1385.
890 Wirth T, and Bernatchez L. 2001. Genetic evidence against panmixia in the European eel. *Nature*
891 409:1037-1040.
892 Wirth T, and Bernatchez L. 2003. Decline of North Atlantic eels: a fatal synergy? *Proceedings of the Royal*
893 *Society of London Series B: Biological Sciences* 270:681-688.
894 Yang Z. 2007. PAML 4: phylogenetic analysis by maximum likelihood. *Molecular Biology and Evolution*
895 24:1586-1591.
896 Yang Z, Wong WS, and Nielsen R. 2005. Bayes empirical Bayes inference of amino acid sites under
897 positive selection. *Molecular Biology and Evolution* 22:1107-1118.

898

Table 1(on next page)

GPS coordinates and summary statistics for each sampling location

The G_ prefix stands for "glass eels". AD2010, AD2011 and AD2012 refer to the th**ree cohorts captured in Adour, France, in the years of 2010, 2011 and 20**12 respectively. The glass eels of BU (Burrishole, (UK), BNIRL (Bann, Nothern Ireland), VSWE (Viskan, Sweden), TENG (Tees, England), EGER (Erms, Germany), OSPA (Oria, Spain), VFRA (Villaine, France), WENG (Wye, England), TITA (Tuscany, Italy), and NIRL (Carlingford, Northern Ireland) were all captured in 2009. All other samples relate to “silver eels”. The remaining acronyms have the following meaning: LC (Larne Lagoon), BT (Bann Toome), Q (Quoile), BU (Burrishole), BL (BannLower), SLC (LoughComber), DK (Denmark), LL (LarneLagoon), SLB (Boretree), GL (Glynn Lagoon), FI (Finland), PT (Portugal), Ger (Germany). N (Number of samples) and respective summary statistics for each location is also shown: nHap (number of haplotypes), S (segregation sites), Hd (Haplotype diversity), π (nucleotide diversity), He (expected heterozygosity), Ho (observed heterozygosity), Ar (Rarefied allelic richness), Fis (Inbreeding coefficient). Values in brackets represent confidence intervals, with the exception of He and Ho, which represents standard deviations* = p<0,05; **=p<0.001.

Population	GPS coordinates	n	nHap	S	*Hd*	π	Tajima-D	He	Ho	Ar	FIS
G_AD2010 (France)	43°31′48″N. 1°31′28″W	155	31	30	0.818 *(0.234-0.859)*	0.00443	-2.3905** *(-1.6033-1.9883)*	0.7343 (0.2689)	0.6177 (0.2440)	2.9	0.1593 *(0.1365 - 0.1760)*
G_AD2011 (France)		129	35	32	0.862 *(0.2965-0.8641)*	0.00514	-2.0896* *(-1.6068-2.1393)*	0.7472 (0.2550)	0.6243 (0.2378)	2.94	0.1650 *(0.1375 - 0.1838)*
G_AD2012 (France)		121	34	35	0.851 *(0.2401-0.8568)*	0.00516	-2.1804** *(-1.5977-2.0335)*	0.7480 (0.2488)	0.6245 (0.2344)	2.94	0.1658 *(0.1398 - 0.1831)*
LC (Ireland)	54°50'54"N. 5°48'51"W	19	4	5	0.7135 *(0.1053-0.8714)*	0.00482	-0.6022 *(-1.7188-1.8481)*	0.7356 (0.2725)	0.5769 (0.2695)	2.91	0.2180 *(0.1319 - 0.2482)*
BT (Ireland)	54°45'23"N. 6°27'48"W	17	9	11	0.8456 *(0.3235-0.9044)*	0.0069	-0.9266 *(-1.7987-1.9496)*	0.7314 (0.2624)	0.6528 (0.2695)	2.88	0.1106 *(0.0251 - 0.1243)*
Q (Ireland)	54°22'0"N. 5°40'4"W	15	5	6	0.6381 *(0.1333-0.8667)*	0.0043	-0.6099 (-1.8159-1.7688)	0.7315 (0.2504)	0.5521 (0.2693)	2.87	0.2537 *(0.1427 - 0.2716)*
BU (N.Ireland)	53°55'4"N. 9°34'20"W	16	4	7	0.575 *(0.1250-0.8833)*	0.0048	-0.6099 *(-1.6965-1.8617)*	0.7477 (0.2662)	0.6367 (0.2537)	2.95	0.1527 *(0.0546 - 0.1761)*
BL (Ireland)	55°9'15"N. 6°42'5"W	11	5	5	0.8364 *(0.1818-0.9091)*	0.00524	-0.6099 *(-1.7116-1.8376)*	0.7060 (0.3007)	0.6152 (0.2611)	2.82	0.1350 *(-0.0315 - 0.1674)*
SLC (Ireland)	54°32'20"N. 5°42'6"W	9	7	7	0.8056 *(0.2222-0.9167)*	0.00612	-0.7082 *(-1.6775-1.7558)*	0.7461 (0.2605)	0.6301 (0.2936)	2.93	0.1606 *(-0.0584 - 0.1802)*
DK (Denmark)	57°29´N. 10°36´E	19	13	16	0.9474 *(0.2924-0.9006)*	0.00703	-1.6199 *(-1.8612-1.9447)*	0.7547 (0.2183)	0.6658 (0.2193)	2.93	0.1208 *(0.0347 - 0.1432)*
LL (Ireland)	54°49'26"N. 5°47'40"W	13	7	6	0.8462 *(0.1539-0.9103)*	0.00545	-0.0199 *(-1.7276-1.7731)*	0.7169 (0.2788)	0.5865 (0.2776)	2.83	0.1884 *(0.0796 - 0.1975)*
SLB (Ireland)	54°26'39"N. 5°35'20"W	15	6	5	0.8476 *(0.1333-0.8667)*	0.00427	-0.0723 *(-1.6850-1.8912)*	0.7462 (0.2648)	0.6025 (0.2653)	2.94	0.1989 *(0.0797 - 0.2264)*
GL (Ireland)	54°49'55N. 5°48'40W	14	10	12	0.9341 *(0.3846-0.9231)*	0.00844	-0.8279 *(-1.7574-1.8956)*	0.7548 (0.2494)	0.6549 (0.2428)	2.96	0.1377 *(0.0057 - 0.1587)*
FI (FInland)	60°26´N; 26°57´E	19	9	9	0.883 *(0.2982-0.8947)*	0.00661	-0.3195 *(-1.6406-1.7888)*	0.735 (0.2600)	0.6348 (0.2547)	2.89	0.1397 *(0.0587 - 0.1621)*
PT (Portugal)	38°46'N. 9°01'W	17	7	8	0.8309 *(0.2279-0.8971)*	0.00644	-0.1299 *(-1.7057-1.9351)*	0.7581 (0.2414)	0.6472 (0.2387)	2.97	0.1397 *(0.0180 - 0.1752)*

Ger (Germany)	54°17'16N. 10°14'54"E	17	6	6	0.7794 *(0.1177-0.8824)*	0.00536	0.2311 *(-1.7057-1.9718)*	0.7328 (0.2516)	0.6041 (0.2586)	2.88	0.1809 *(0.0779 - 0.2012)*
G_BU (NIreland)	53°55'4"N. 9°34'20"W	14	6	6	0.78 *(0.1429-0.9011)*	0.00494	-0.26534 *(-1.6705-1.6921)*	0.7224 (0.2741)	0.6294 (0.272)	2.85	0.1332 *(0.0309 - 0.1508)*
G_BNIRL (NIreland)	55°9'15"N. 6°42'5"W	12	8	9	0.909 *(0.3030-0.9242)*	0.00629	-1.02555 (-1.7551-1.7575)	0.7224 (0.2741)	0.6294 (0.2720)	2.81	0.1635 *(0.0209 - 0.2125)*
G_VSWE (Sweden)	57°13'30"N. 12°12'20"E	16	8	7	0.00433 *(0.1250-0.8750)*	0.00433	-0.96247 *(-1.7280-1.9375)*	0.7432 (0.2700)	0.6335 (0.2946)	2.93	0.1518 *(0.0618 - 0.1637)*
G_TENG (England)	54°37'21"N. 1°9'23"W	10	7	7	0.911 *(0.0000-0.9111)*	0.00515	-1.11638 *(-1.7118-1.6872)*	0.7402 (0.2584)	0.6591 (0.2404)	2.9	0.1160 *(-0.0810 - 0.1260)*
G_EGER (Germany)	48°35'35"N. 9°14'11"E	5	4	3	0.9 *(0.0000-0.9000)*	0.00395	-0.17475 *(-1.4554-1.6407)*	0.7111 (0.2951)	0.6000 (0.3086)	2.82	*0.1724 (-0.2152 - 0.1724)*
G_OSPA (Spain)	43°17'25"N. 2° 7'55"W	4	3	2	0.833 *(0.0000-1.0000)*	0.00282	-0.7099 *(-0.7968-2.0118)*	0.7265 (0.2894)	0.6705 (0.3483)	2.85	0.0876 *(-0.3333 - 0.0876)*
G_VFRA (France)	47°30'20"N. 2°29'57"W	3	2	2	0.667 *(0.0000-1.0000)*	0.00377	- -	0.7439 (0.2442)	0.6970 (0.2800)	2.88	0.0800 *(-1.0000 - 0.0800)*
G_WENG (England)	51°36'36"N. 2°39'43"W	5	4	4	0.9 *(0.0000-1.0000)*	0.00565	0.27345 *(-1.1743-1.6859)*	0.7323 (0.2221)	0.6455 (0.2686)	2.83	0.1315 *(-0.2840 - 0.1315)*
G_TITA (Italy)	43° 40' 47" N. 10° 16' 36" E	4	3	3	0.833 *(0.0000-1.0000)*	0.00471	0.16766 *(-0.8173-2.0118)*	0.7175 (0.3169)	0.5568 (0.3444)	2.85	0.2519 *(-0.2609 - 0.2519)*
G_NIRL (NIreland)	54.07°N. 6.19°W	3	3	3	1 *(0.0000-1.0000)*	0.00563	- -	0.6869 (0.2787	0.6636 (0.3513)	2.71	0.0379 *(-0.3398 - 0.0597)*

1

Table 2(on next page)

Molecular indices of "s*ilver eels*" and "*glass eels*"

Summary statistics of neutral evolving markers calculated for the two distinct generations. n = number of samples used; nHap = number of haplotypes; S = segregation sites; Hd = Haplotype diversity; π = nucleotide diversity; He = expected heterozygosity; Ho observed heterozygosity; Ar = Rarefied allelic richness; Fis = Inbreeding coefficient; Values in brackets represent confidence intervals, with the exception of He and Ho which represents standard deviations* = p<0,05; **=p<0.001

Populatio n	n	nHap	S	*Hd*	*π*	Tajima-D	He	Ho	Ar	FIS
silver eels	202	34	33	0.821 *(0.2230-0.8423)*	0.00481	-2.05326 *(-1.6500-1.9464)*	0.7438 (0.2528)	0.6233 (0.2376)	11.74	0.1649 *(0.1450 - 0.1802)*
glass eels	481	85	65	0.842 *(0.1941-0.843)*	0.00489	-2.35741 *(-1.5842-1.94939)*	0.7427 (0.2598)	0.6215 (0.2304)	11.83	0.1610 *(0.1488 - 0.1710)*

Table 3 (on next page)

MHC molecular indices for "*silver eels*" and "*glass eels*"

Summary statistics of the MHC calculated for the two distinct generations. nHap = number of haplotypes; S = segregation sites; Hd = Haplotype diversity; π = nucleotide diversity; k = average number of differences; nr alleles/ind = average number alleles per individual with respective standard error (se); dist_nt = average nucleotide distance per individual with respective standard error (se); R = recombination rate; θ = mutation rate; Rm = minimum number of recombination events detected; R/θ = ratio of recombination and mutation.

Life Stage	nAlleles	nIndividuals	nHap	S	*h*	π	nr alleles/ind	se	dist_nt	se	R	θ	Rm	R/θ
					0.981							22.983		
glass eels	332	97	115	100	1	0.1179	3.423	0.166	0.117	0.006	48.0000	0	10	2.0885
					0.982							24.385		
silver eels	654	230	184	115	0	0.1232	2.856	0.101	0.101	0.004	53.0000	0	11	2.1735

1

Figure 1(on next page)

Location-specific demography accessed with neutral evolving markers

Two types of analyses specific to each marker are presented in this figure: mismatch pairwise distribution of mtDNA's single nucleotide polymorphisms within locations a) (top), and frequency distribution of allelic states across microsatellite loci b) (bot). The locations here exposed are G_AD2010 (cohort of 2010 from Adour), BU (Burrishole), SLC (LoughComber), Q (Quoile) and were chosen among the others in order to show the variety of demographic signatures produced by mtDNA data. Therefore in mismatch pairwise distribution graphs, full blue lines represent expected distribution under sudden population expansion, full red lines represent expected distribution under constant population size and dotted lines the observed distribution. The x-axis shows the number of mismatches and y-axis its frequency. It is possible to observe the signature of an expanding population in G_AD2010, stable population or recovery from bottleneck BU and SLC, and stable population in Q. Allele frequency distribution plots obtained from same locations show the signature of non-bottlenecked population b) (bot). In these graphs, the bars correspond to allele frequencies, x-axis corresponds to allele frequency classes and y-plots to number of alleles.

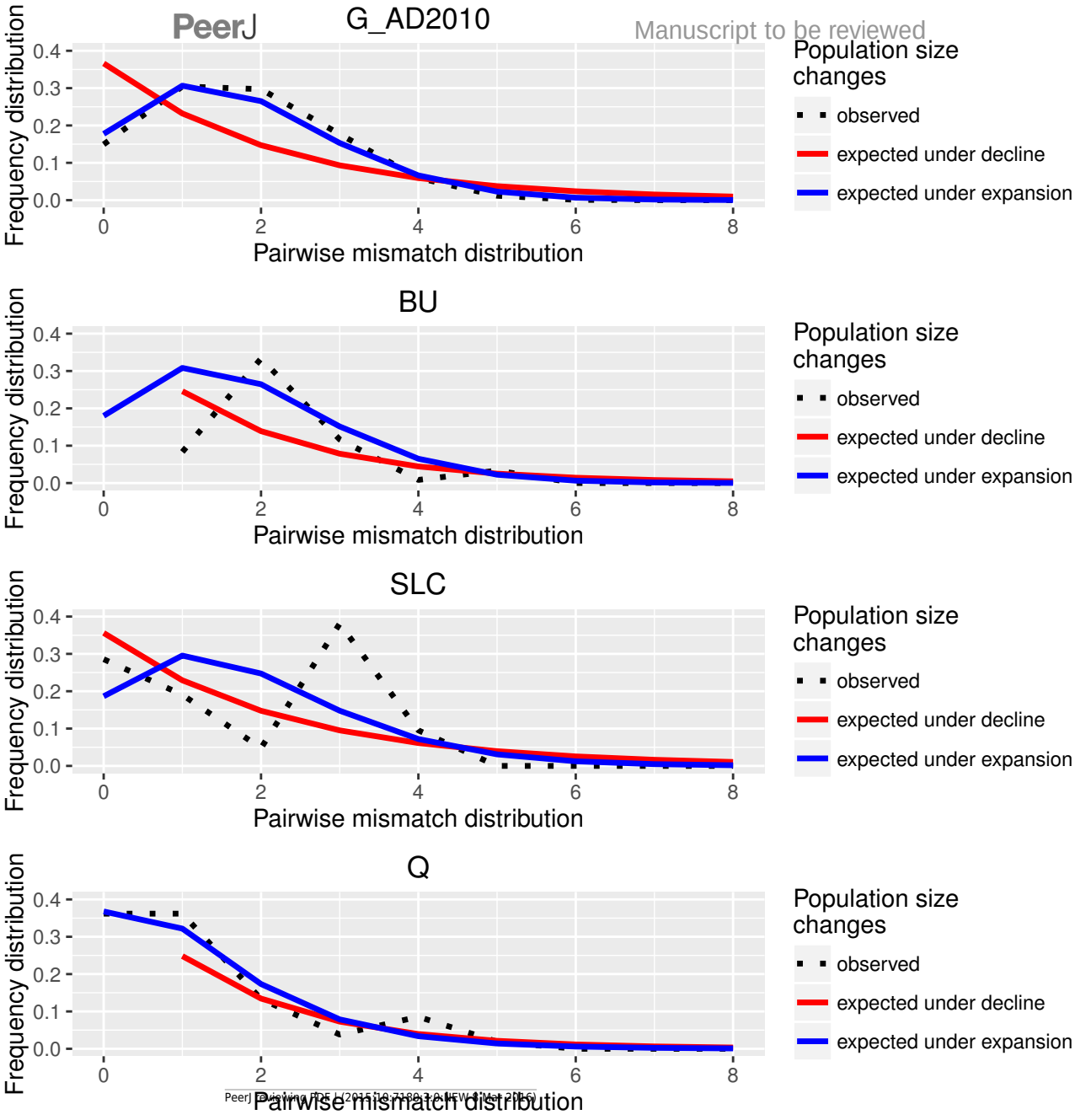
G_AD2010
Frequency distribution
Pairwise mismatch distribution
Population size changes
observed
expected under decline
expected under expansion
BU
Frequency distribution
Pairwise mismatch distribution
Population size changes
observed
expected under decline
expected under expansion
SLC
Frequency distribution
Pairwise mismatch distribution
Population size changes
observed
expected under decline
expected under expansion
Q
Frequency distribution
Pairwise mismatch distribution
Population size changes
observed
expected under decline
expected under expansion

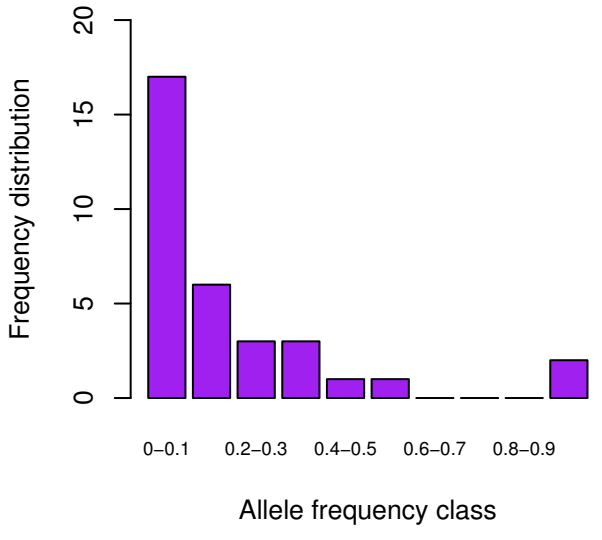
G_AD2010
Frequency distribution
0
5
10
15
20
0–0.1
0.2–0.3
0.4–0.5
0.6–0.7
0.8–0.9
Allele frequency class

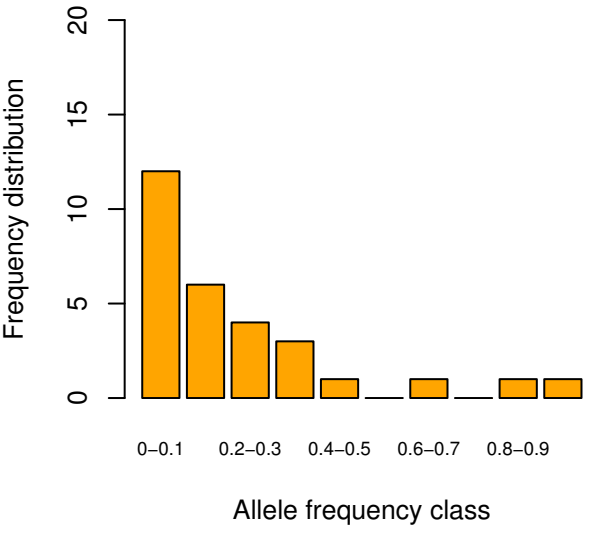
BU
Frequency distribution
0
5
10
15
20
0–0.1
0.2–0.3
0.4–0.5
0.6–0.7
0.8–0.9
Allele frequency class

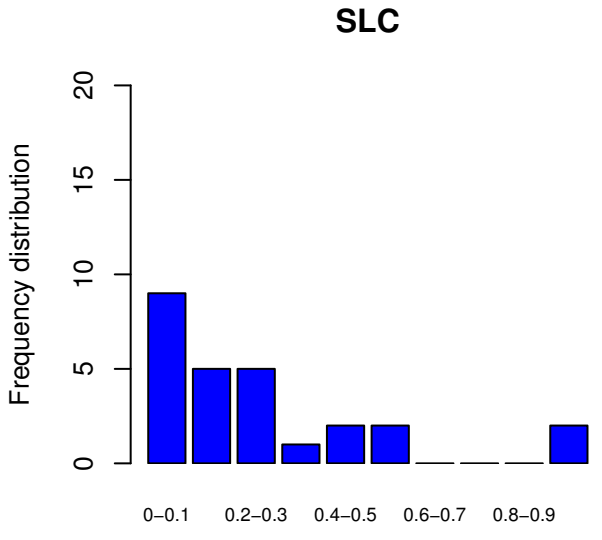
SLC
Frequency distribution
0
5
10
15
20
0–0.1
0.2–0.3
0.4–0.5
0.6–0.7
0.8–0.9
Allele frequency class

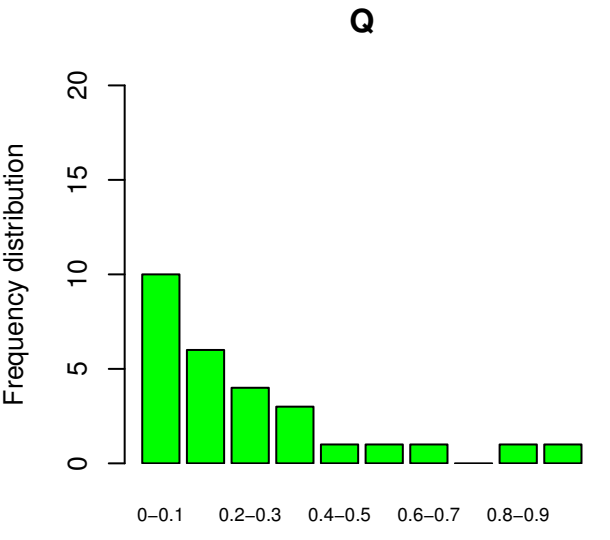
Q
Frequency distribution
0
5
10
15
20
0–0.1
0.2–0.3
0.4–0.5
0.6–0.7
0.8–0.9
Allele frequency class

Figure 2(on next page)

Species and cohort-based demography accessed with neutral evolving markers

Mismatch pairwise distribution of mtDNA's single nucleotide polymorphisms considering both the full data set (top graph) and each generation separately. Here also, the full blue lines represent expected distribution under sudden population expansion, full red lines represent expected distribution under constant population size and dotted lines the observed distribution. All distributions showed a typical signature of expansion.

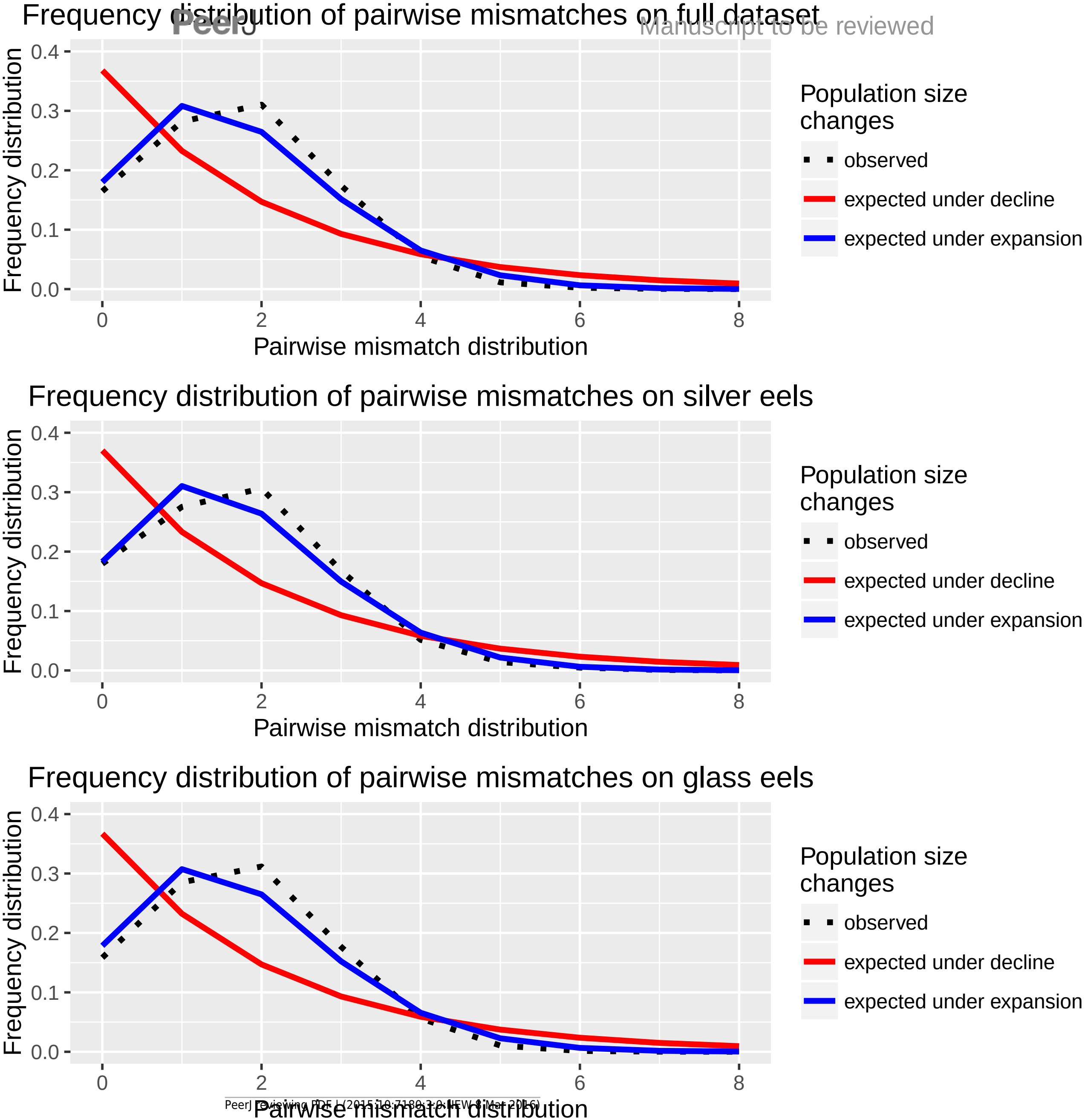
Frequency distribution of pairwise mismatches on full dataset
Frequency distribution
Pairwise mismatch distribution
Population size changes
observed
expected under decline
expected under expansion
Frequency distribution of pairwise mismatches on silver eels
Frequency distribution
Pairwise mismatch distribution
Population size changes
observed
expected under decline
expected under expansion
Frequency distribution of pairwise mismatches on glass eels
Frequency distribution
Pairwise mismatch distribution
Population size changes
observed
expected under decline
expected under expansion

Figure 3(on next page)

Landmarks in the allelic sequence of exon 2 of MHC class II B of the European eel.

a) Aminoacid alignment with human HLA-DRB1. For simplification purposes, only some of the alleles are shown. + denotes human antigen binding sites, - T cell receptor contact sites and * sites that putatively interact with both. Sites estimated to be experiencing or have experienced positive selection are highlighted in green (identified by CODEML only), red (identified by MEME only) and blue (identified by both methods). b) Sliding window graph of ψ. Measures of the probability (ψ) of a site being informative of conversion event in relation to the position in the alignment (in base pairs). Here it is possible to observe the two gene conversion tracts detected amongst “glass eels”, i.e. the regions 137-141 and 166-168.

a)

```
                 1                   22                  44                  66
Anan-DXB0        QDLEFIDRYI FNKLEYARYN STLNKFIGYT EHGVKNADRW N-RDGEAERQ HANLDSYCRH NAEL--SFN
Anan-DXB1        .....L.... .....LL... .....L.... AL..Q....L .-...S..G. .T...G...P ....--..R
Anan-DXB2        ......L..V ......G... .....Y.... .......E.F .-.....D.. .T...G...P ....--..R
Anan-DXB3        ....Y.S... ......I... .....L.... .L...H.EI. .-...S..QT .TY..G.... ....--...
Anan-DXB4        .....L.... .....L.... .....L.... .F..... .-...G.... .....G.... ....--...
Anan-DXB5        .....L.... .....L.... .....L.... ..... .-.....D.. .T...G.... ....--...
Anan-DXB6        ......S..V ......L... .....L.... .....E.A .-QE..P... .....G..KP ....--..R
Anan-DXB7        .....L.... .....L.... .....L.... .F.....EI. .-K..S..QT .....G.... ....--...
Anan-DXB8        ......N.Q. .....FL... .....L.... .L.....L .-.E..P... .....G..KP ....--..R
Anan-DXB9        ....Y.G... .....L.... .....V.... D.....E.L .-..... .....A...P ...S--...
Anan-DXB10       .....L.... .....FL... .....L.... .L.....EIF .-Q..STD.. .I..EG.... ....--...
#DRB1*010101     ERVRLLE.C. Y.QE.SV.FD .DVGEYRAV. .L.RPD.EY. .SQKDLL.QR R.AV.T.... .YGVGE..T
                    +++  +      ++         +         ++  -+   - -* --* --+ --++ - +  ++  ++
```

b)

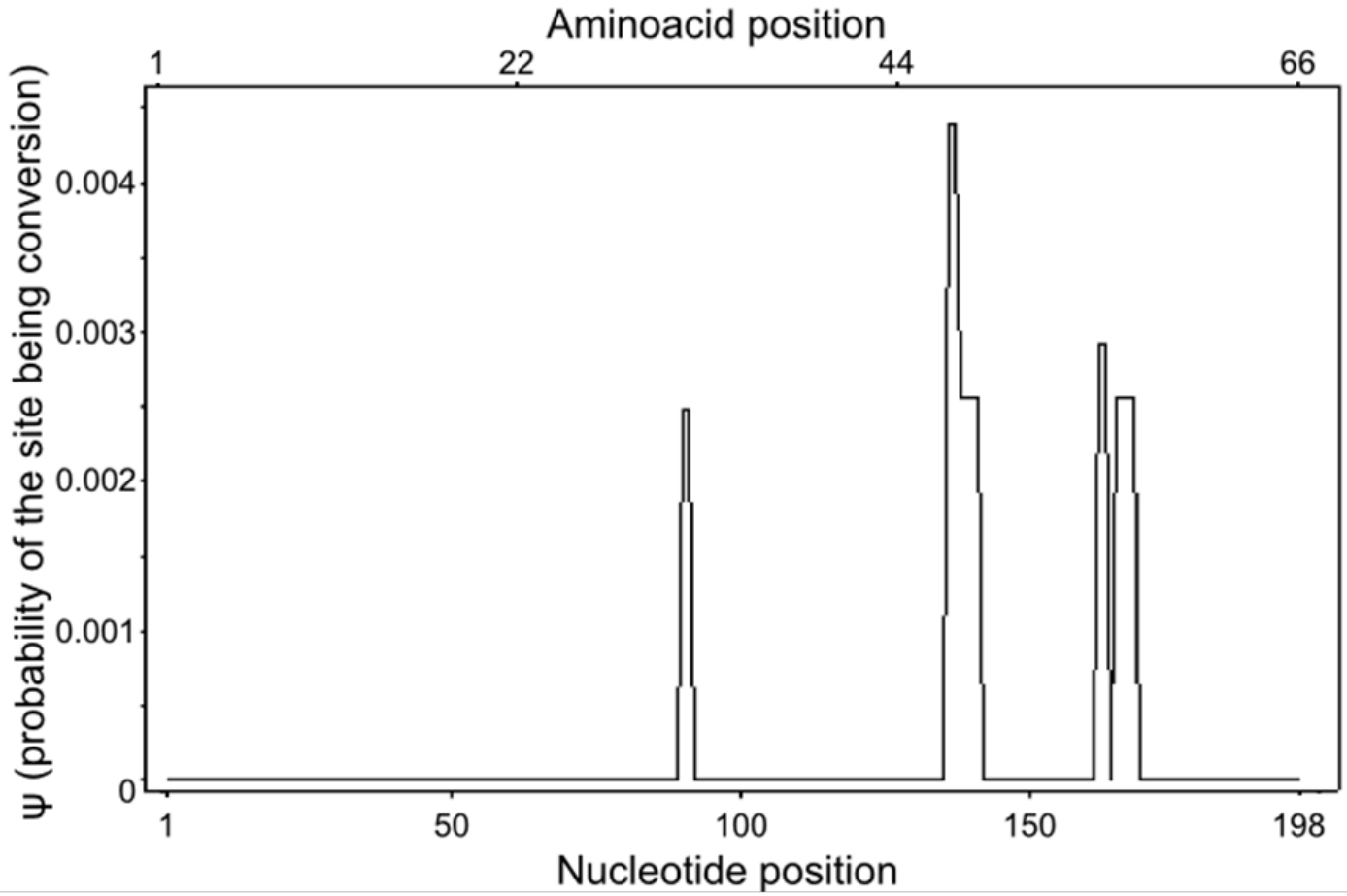

Figure 4(on next page)

Historical profile of MHCs genetic diversity considering the positively selected sites (PSS) of the exon 2 of MHC class II B.

Above are the observed mismatch distributions of a) “glass eels” and b) “silver eels” (dotted lines) plotted against expected distribution of a population expansion (full lines). Below are the Bayesian skyline plots of “glass eels”, considering 0.2 substitutions/ unit of time, c), 1 substitution/unit of time, e), and 5 substitutions/unit of time, g). On the right, Bayesian skyline plots of “silver eels”, considering 0.2 substitutions/ unit of time, d), 1 substitution/unit of time, f), and 5 substitutions/unit of time, h). X-axis represents “time”. The lack of a clock-like evolution did not allow the definition of a time unit. Y-axis is an estimate of the product of Ne * mutation rate (μ) per unit of time. The black like represents the mean Ne and the blue shading the 95% HPD (high probability density) interval.

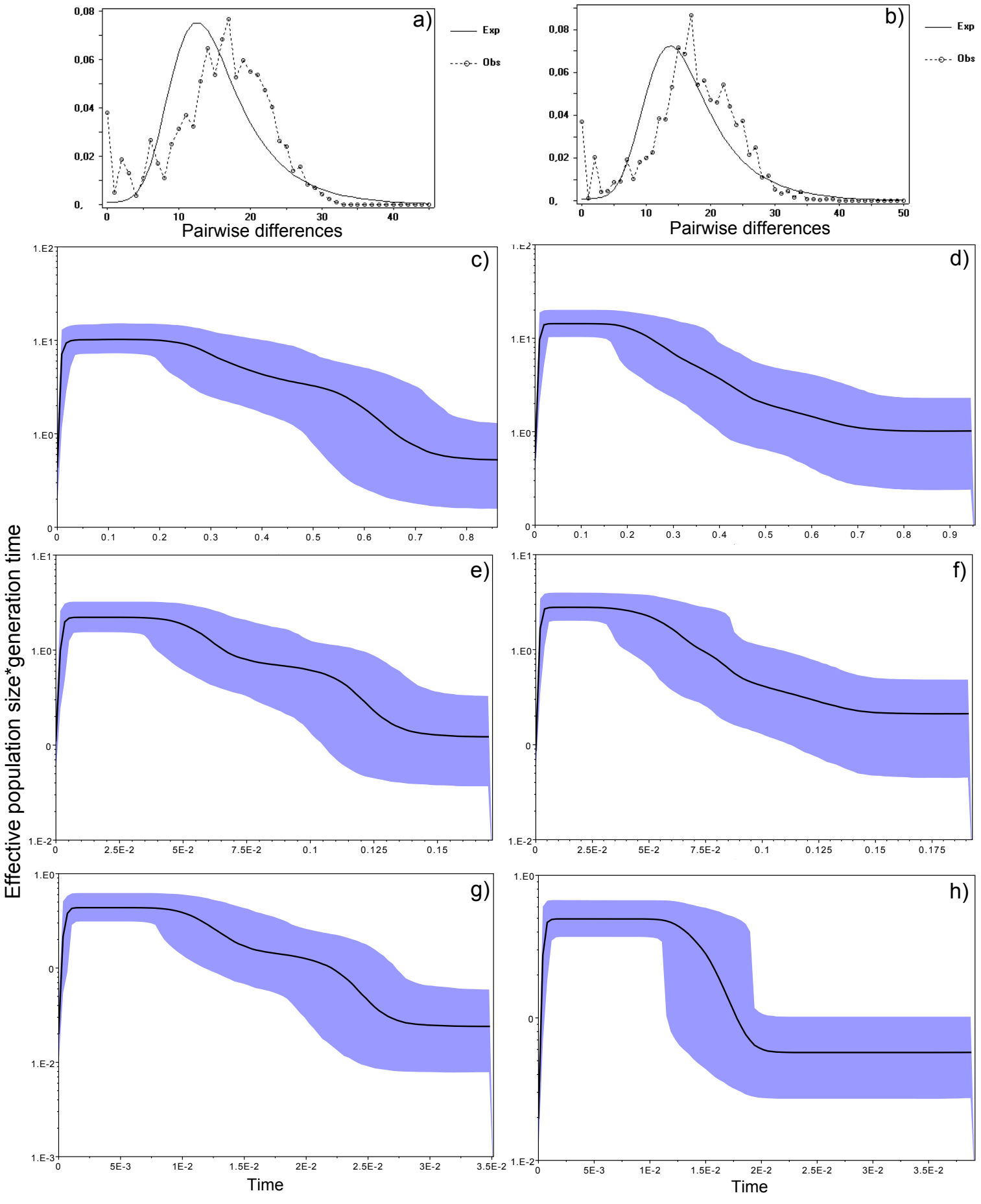
a)
Exp
Obs
Pairwise differences
b)
Exp
Obs
Pairwise differences
c)
d)
e)
f)
g)
h)
Effective population size*generation time
Time
Time

Figure 5(on next page)

Historical profile of MHCs genetic diversity considering the non-positively selected sites (nPSS) of the exon 2 of MHC class II B

Above are the observed mismatch distributions of a) “glass eels” and b) “silver eels” (dotted lines) plotted against expected distribution of a population expansion (full lines). Below, are the Bayesian skyline plots of “glass eels”, considering 0.2 substitutions/ unit of time, c), 1 substitution/unit of time, e), and 5 substitutions/unit of time, g). On the right, Bayesian skyline plots of “silver eels”, considering 0.0002 substitutions/ unit of time, d), 1 substitution/unit of time, f) , and 5 substitutions/unit of time, h).

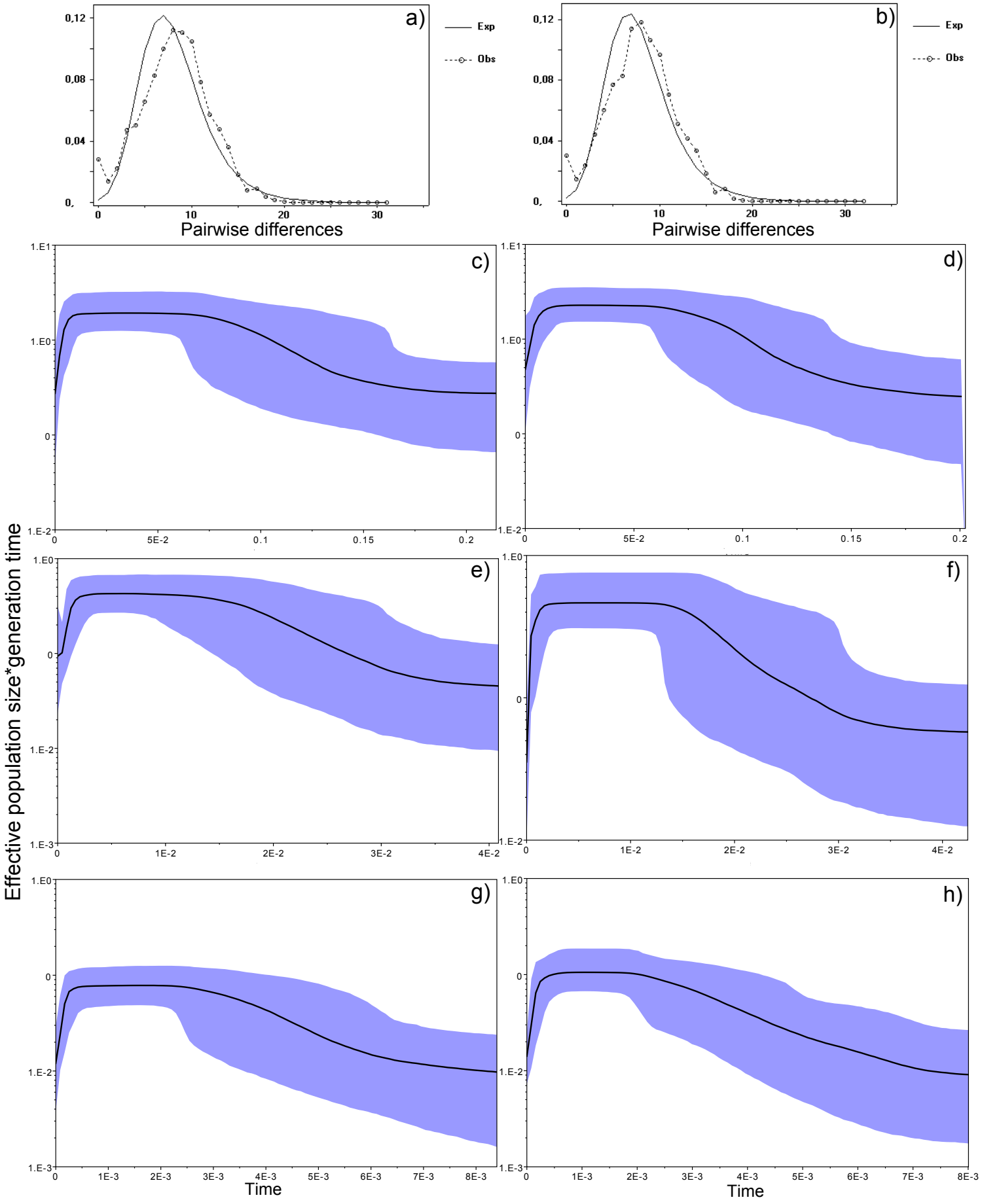
a)
b)
Exp
Obs
Pairwise differences
c)
d)
e)
f)
g)
h)
Effective population size*generation time
Time

Figure 6(on next page)

Lineages-through-time plots (LTT)

Lineage diversification for a) “silver eels” and b) ”glass eels”, with both graphs showing a recent burst of lineage diversification. These graphs were built with PSS using the substitution rate of 5. Like in Bayesian skyline plots, no unit of time is defined. The y-axis represents the number of lineages through time.

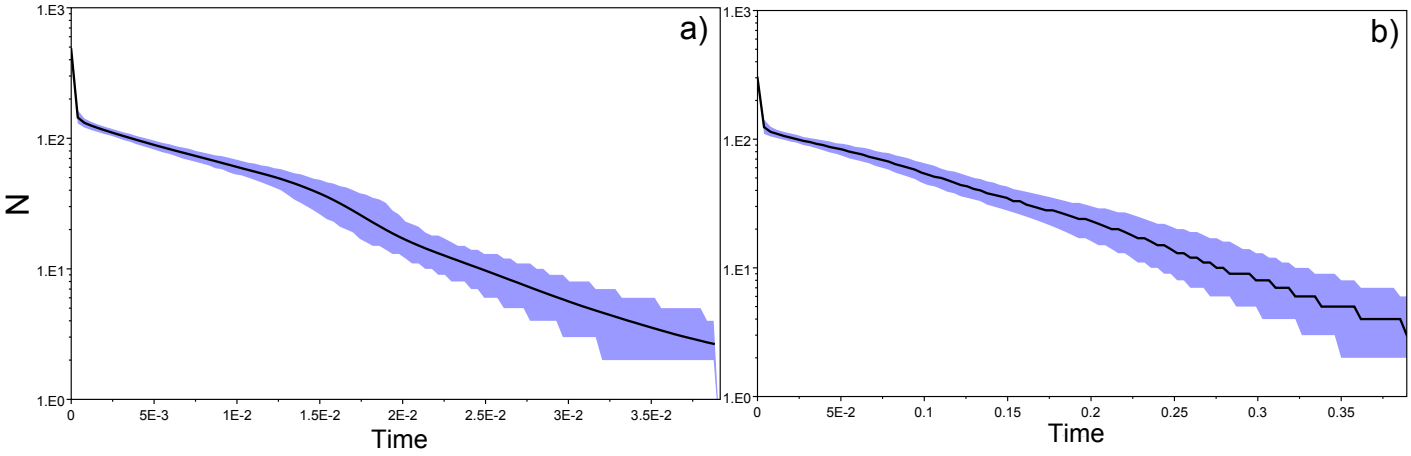
a)
b)
N
1.E3
1.E2
1.E1
1.E0
0
5E-3
1E-2
1.5E-2
2E-2
2.5E-2
3E-2
3.5E-2
5E-2
0.1
0.15
0.2
0.25
0.3
0.35
Time
Time